



Article

Thymoquinone, a Novel Multi-Strike Inhibitor of Pro-Tumorigenic Breast Cancer (BC) Markers: CALR, NLRP3 Pathway and sPD-L1 in PBMCs of HR+ and TNBC Patients

Sawsan Elgohary ¹, Reda A. Eissa ² and Hend M. El Tayebi ^{1,*}

¹ Clinical Pharmacology and Pharmacogenomics Research Group, Department of Pharmacology and Toxicology, Faculty of Pharmacy and Biotechnology, German University in Cairo, Cairo 11835, Egypt; sawsanelgohary54@gmail.com

² Department of Surgery, Faculty of Medicine, Ain Shams University, Cairo 11591, Egypt; reissa75@gmail.com

* Correspondence: hend.saber@guc.edu.eg; Tel.: +20-1005566415; Fax: +20-2-27581041

Abstract: Breast cancer (BC) is not only a mass of malignant cells but also a systemic inflammatory disease. BC pro-tumorigenic inflammation has been shown to promote immune evasion and provoke BC progression. The NOD-like receptor (NLR) family pyrin domain-containing protein 3 (NLRP3) inflammasome is activated when pattern recognition receptors (PRRs) sense danger signals such as calreticulin (CALR) from damaged/dying cells, leading to the secretion of interleukin-1 β (IL-1 β). CALR is a novel BC biological marker, and its high levels are associated with advanced tumors. NLRP3 expression is strongly correlated with an elevated proliferative index Ki67, BC progression, metastasis, and recurrence in patients with hormone receptor-positive (HR+) and triple-negative BC (TNBC). Tumor-associated macrophages (TAMs) secrete high levels of IL-1 β promoting endocrine resistance in HR+ BC. Recently, an immunosuppressive soluble form of programmed death ligand 1 (sPD-L1) has been identified as a novel prognostic biomarker in triple-negative breast cancer (TNBC) patients. Interestingly, IL-1 β induces sPD-L1 release. BC Patients with elevated IL-1 β and sPD-L1 levels show significantly short progression-free survival. For the first time, this study aims to investigate the inhibitory impact of thymoquinone (TQ) on CALR, the NLRP3 pathway and sPD-L1 in HR+ and TNBC. Blood samples were collected from 45 patients with BC. The effect of differing TQ concentrations for different durations on the expression of CALR, NLRP3 complex components and IL-1 β as well as the protein levels of sPD-L1 and IL-1 β were investigated in the peripheral blood mononuclear cells (PBMCs) and TAMs of TNBC and HR+ BC patients, respectively. The findings showed that TQ significantly downregulated the expression of CALR, NLRP3 components and IL-1 β together with the protein levels of secreted IL-1 β and sPD-L1. The current findings demonstrated novel immunomodulatory effects of TQ, highlighting its potential role not only as an excellent adjuvant but also as a possible immunotherapeutic agent in HR+ and TNBC patients.

Keywords: thymoquinone; PRR; calreticulin; NLRP3; PYCARD; caspase-1; IL-1 β ; sPD-L1; triple-negative breast cancer; hormone receptor-positive breast cancer



Citation: Elgohary, S.; Eissa, R.A.; El Tayebi, H.M. Thymoquinone, a Novel Multi-Strike Inhibitor of Pro-Tumorigenic Breast Cancer (BC) Markers: CALR, NLRP3 Pathway and sPD-L1 in PBMCs of HR+ and TNBC Patients. *Int. J. Mol. Sci.* **2023**, *24*, 14254. <https://doi.org/10.3390/ijms241814254>

Academic Editors: Patrick Ming-Kuen Tang and Dongmei Zhang

Received: 16 May 2023

Revised: 19 June 2023

Accepted: 25 June 2023

Published: 19 September 2023



Copyright: © 2023 by the authors. Licensee MDPI, Basel, Switzerland. This article is an open access article distributed under the terms and conditions of the Creative Commons Attribution (CC BY) license (<https://creativecommons.org/licenses/by/4.0/>).

1. Introduction

In 2020, breast cancer (BC) was ranked the most diagnosed cancer and the fifth-highest cause of cancer mortality worldwide [1]. Five molecular BC subtypes have been extensively characterized, comprising luminal A, with the best prognosis; luminal B/human epidermal growth factor receptor-negative (HER2-); luminal B/HER2+; HER-2 enriched [2]; and finally the most aggressive triple-negative breast cancer (TNBC) subtype, which lacks targeted therapy [2]. It has been shown that BC is not only an autonomous mass of epithelial cells but also a systemic inflammatory disease and a serious consequence of chronic inflammation [3–5]. Peripheral blood represents reservoirs and activation sites of immune cells during BC progression [6]. Interestingly, the protein expression profile

of peripheral blood mononuclear cells (PBMCs) has been shown to be a reflection of its expression within the BC tissue itself [7]. Cancer cells perturb gene expression in PBMCs, leading to many systemic signaling and immune evasion issues in BC patients [8]. In tumor microenvironment, distinct inflammatory proteins and immune cells release various cytokines into the bloodstream, promoting systemic inflammation [9]. These chronic inflammatory actions may be triggered by danger signals called danger-associated molecular patterns (DAMPs) released from injured or dying cells, leading to the initiation of sterile inflammation and immunogenic cell death (ICD) [10,11]. TNBC is the most immunogenic subtype [12,13], while estrogen receptor + (ER+) BC, specifically luminal A, is the least immunogenic subtype [14]. Failure of DAMPs to generate an effective antitumor response might turn DAMPs into a tumor-promoting mechanism and enhance chronic inflammation [10,15]. DAMPs represent a large range of chemically unrelated mediators, such as calreticulin (CALR) and adenosine triphosphate (ATP) [16]. In healthy cells, CALR resides in the endoplasmic reticulum (ER), acting as a chaperone that corrects protein folding [17]. Various chemotherapeutics [18], radiation [19], and oncolytic peptides [20] induce CALR's translocation to the cell surface, acting as a DAMP and producing an "eat-me signal" that stimulates the engulfment of apoptotic cells by phagocytes [21]. CALR is expressed in PBMCs, including activated peripheral blood T-cells [22], macrophages [23], immature DC, monocytes [24], plasma cells [25], and NK cells [26]. Interestingly, the exposed CALR has been shown to be subsequently released and detected in the extracellular milieu [27]. Recently, CALR has been addressed as a promising biological marker of BC and an indicator of BC staging and prognosis [28–32]. In addition, the literature reported that CALR expression was associated with more advanced tumors in a study of 228 BC samples [33]. Moreover, in a cohort of 33 patients with BC, high levels of CALR correlated with metastasis, especially in axillary lymph nodes [31], and mediated the invasive BC phenotype [34].

Inflammasomes are inflammatory signaling complexes made up of pattern recognition receptors (PRRs) that sense released DAMPs, leading to their oligomerization recruiting the apoptosis-associated speck-like protein containing a caspase recruitment domain (ASC) also called PYCARD (PYD and CARD domain-containing) and the effector caspase-1 [35], which then cleaves the pro-interleukin-1 β (pro-IL-1 β) into the mature active IL-1 β [35]. The NOD-like receptor (NLR) family pyrin domain-containing protein 3 (NLRP3) is the most extensively studied inflammasome [35]. Numerous studies have demonstrated that CALR is an NLRP3 activator [36–39]. NLRP3 is expressed in PBMCs [40,41], including B-cells, T-cells, dendritic cells, monocytes (very weakly) [42,43], and macrophages [44]. NLRP3 hyperactivation in PBMCs is exhibited in various inflammatory diseases [45–51], distinct cardiovascular diseases [52–55], and enhanced systemic inflammatory states [52], and it was detected in PBMCs of postmortem coronavirus disease-19 (COVID-19) patients [56]. In addition, NLRP3 was found to be overexpressed in PBMCs of various cancer patients [57–60]. In BC, the clinical analysis showed that NLRP3 and PYCARD expressions were strongly associated with more aggressive clinicopathological factors such as tumor size and proliferative index Ki67 and contributed to BC progression, especially in luminal BC patients [61]. Furthermore, claudin-low BC patients displayed an elevated expression of NLRP3, which was correlated with poor survival [62]. In addition, NLRP3 activation promoted BC metastasis and contributed to immune system dysfunction [63,64].

IL-1 β is one of the primary mediators of systemic inflammation [65]. Distinct studies detected its expression in PBMCs [65–68]. In patients with invasive BC, IL-1 β production by peripheral blood cells was associated with lymphatic metastasis [69]. Enzyme-linked immunosorbent assay (ELISA) findings showed that IL- β expressions were significantly increased in the sera and plasma of BC patients compared to the control group [70,71] and were related to tumor size, clinical stage, histological grade, and lymph node metastasis [70]. In addition, patients with metastatic BC exhibited an increased production of IL-1 β compared to patients with early BC [72]. Macrophages, particularly tumor-associated macrophages (TAMs), are one of the main cell types that secrete high levels of IL-1 β [73,74],

promoting endocrine- and chemo-resistance in ER+ BC [75–77] through significantly decreasing ER α levels [76].

Tumor evasion has been a critical characteristic of cancer progression and poor prognosis in TNBC [12,78,79]. The immune checkpoint programmed death-1 (PD-1), which is expressed on activated T-cells [80], acts as “brakes” that protect against autoimmunity [81] via binding to its ligand, programmed death ligand 1 (PD-L1), subsequently delivering inhibitory signals to T-cells, which leads to its exhaustion and deactivation [82]. Surprisingly, tumor cells not only express PD-L1 on its surface, but also secrete a soluble form of PD-L1 (sPD-L1) with an immunosuppressive function [83] that can be generated by cleavage from the cell surface [84]. Lately, sPD-L1 has attracted much attention [85], and emerging evidence has addressed sPD-L1 as a marker of inflammation [86]. In 2021, findings manifested a significant correlation between tumoral PD-L1 and sPD-L1 in the serum of BC patients [87]. A recent study reported that sPD-L1 could be used as a noninvasive biomarker for evaluating the malignancy of TNBC [88] since its high serum levels were correlated with poor response to neoadjuvant chemotherapy in patients with TNBC [88]. The results of another study agreed with these findings, showing that high levels of sPD-L1 in peripheral blood were associated with poor prognosis in BC [87]. These outcomes were further confirmed in March 2021, when it was stated that plasma sPD-L1 levels were higher in recurrent/metastatic patients than those in early-stage patients [87]. Yongjing Chen et al. reported that sPD-L1 was detected in the supernatant of MDA-MB231 [84]. Interestingly, a study in 2023 showed that IL-1 β induced sPD-L1 release and enhanced membrane PD-L1 levels [86]. BC patients with elevated IL-1 β and sPDL-1 levels showed a significantly shorter progression-free survival [89].

Thymoquinone (TQ) is a natural pharmacologically active ingredient derived from *Nigella sativa* seeds [90]. It has been known for its chemo-preventive and antineoplastic effects in diverse types of cancer for more than 50 years, as reviewed by our research group [91]. In BC, TQ exerted cytotoxic effects against various BC cell lines [92–97] and showed selective cytotoxicity against BC cells compared to normal cells [98]. Another study confirmed these results, demonstrating that TQ exerted selective cytotoxicity against pancreatic cancer cell lines compared to the non-toxic effect against PBMCs even at 100 μ M [99]. In addition, TQ showed proliferative effects and enhanced immunological properties in PBMCs and macrophages, respectively [99,100]. To date, no literature explored the impact of TQ on CALR expression in any study model or ailment. Recently, few studies investigated the inhibitory effect of TQ on the NLRP3 pathway in distinct *in vivo* and *in vitro* models [101–106]. In addition, a recent study showed that TQ significantly inhibited the protein expression of PD-L1 in the TNBC cell line [107]. In contrast, TQ’s inhibitory effects on inflammasome and sPD-L1 are not explored yet in BC. This study is the first to explore whether TQ could target the aforementioned pro-tumorigenic BC markers, which consist of the CALR, NLRP3 pathway with a focus on the downstream IL-1 β expression and protein release in both PBMCs and TAMs isolated from TNBC and HR+ BC patients, respectively. The second purpose was to compare the protein levels of sPD-L1 in HR+ and TNBC patients. Finally, the inhibitory effect of TQ on sPD-L1 was further investigated. Overall, this study was performed using different TQ concentrations for distinct durations.

2. Results

2.1. TQ-Inhibited CALR in PBMCs of HR+ BC Patients

PBMCs isolated from HR+ BC patients were treated with increasing concentrations of TQ (20, 50, and 100 μ M) for 24, 48, and 72 h. CALR expression was investigated compared to that of the DMSO control, and each concentration was performed in triplicate. After 24 h of TQ treatment, the 20 μ M concentration resulted in a non-significant elevation in CALR expression. In contrast, the 50 μ M (* p = 0.0195) and 100 μ M (** p = 0.0013) concentrations significantly downregulated its expression (one-way analysis of variance (ANOVA), **** p < 0.0001; Figure 1A). After 48 h, the results showed a dose-dependent inhibition, which was significant at 50 μ M (* p = 0.0345) and 100 μ M (** p = 0.0043) (one-way

ANOVA, $** p = 0.0033$; Figure 1B). TQ significantly downregulated the expression of CALR at 20 μM ($* p = 0.0414$), 50 μM ($* p = 0.0184$), and 100 μM ($* p = 0.0154$) concentrations after 72 h of treatment (one-way ANOVA, $** p = 0.0045$; Figure 1C).

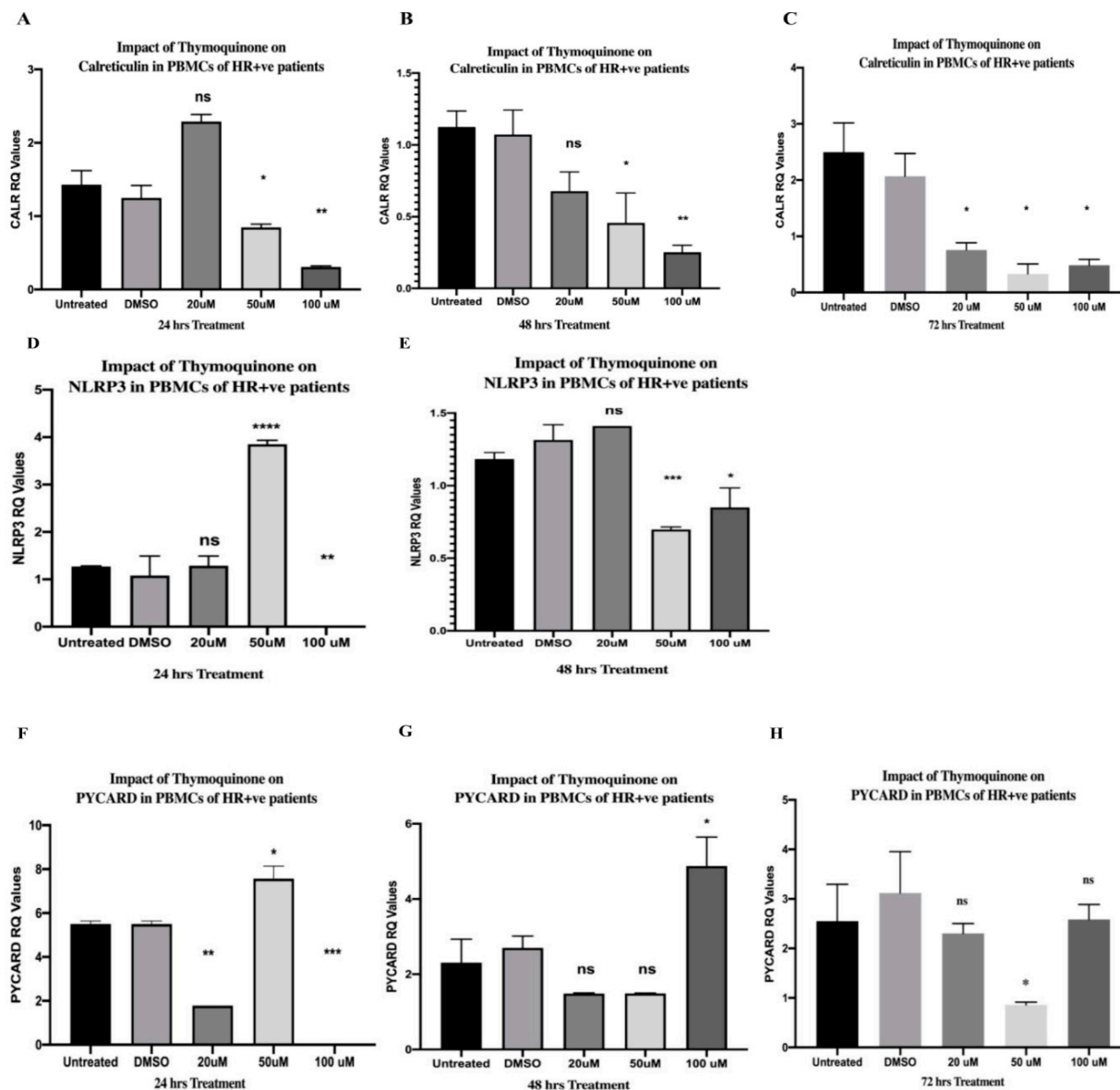


Figure 1. Inhibitory impact of TQ on CALR, NLRP3 and PYCARD expression in PBMCs of HR+ BC patients. (A–C) CALR expression versus TQ concentrations. PBMCs isolated from HR+ BC patients were treated with TQ (0, 20, 50, and 100 μM) for (A) 24 h, (B) 48 h, and (C) 72 h. (D–E) NLRP3 expression versus TQ concentrations. PBMCs isolated from HR+ BC patients were treated with TQ (0, 20, 50, and 100 μM) for (D) 24 h and (E) 48 h. (F–H) PYCARD expression versus TQ concentrations. PBMCs isolated from HR+ BC patients were treated with TQ (0, 20, 50, and 100 μM) for (F) 24 h, (G) 48 h, and (H) 72 h. All experiments were performed in triplicate, and data are expressed as the mean \pm standard deviation. Statistical analysis was performed using the GraphPad Prism software version 9.1.1. The data were analyzed using one-way ANOVA and Dunnett’s multiple comparisons to compare each treated column and the DMSO control column (**** p value < 0.0001 ; *** p value < 0.001 ; ** p value < 0.01 ; * p value < 0.05). TQ: thymoquinone; CALR: calreticulin; NLRP3: NOD-like receptor (NLR) family pyrin domain-containing protein 3 (NLRP3); PYCARD: PYD and CARD domain containing; PBMCs: peripheral blood mononuclear cells; HR+: hormone receptor-positive; BC: breast cancer; DMSO: dimethyl sulfoxide; ns: non-significant.

2.2. TQ Significantly Downregulated CALR Expression in PBMCs Isolated from TNBC Patients in a Dose-Dependent Manner

TQ showed strong significant inhibition on the CALR expression after 24 h of treatment at 20 μM (**** $p < 0.0001$), 50 μM (**** $p < 0.0001$), and 100 μM (**** $p < 0.0001$) in a dose-dependent manner (one-way ANOVA, **** $p < 0.0001$) (Figure 2A). After 48 h of treatment, TQ significantly inhibited the expression of CALR at 20 μM (* $p = 0.0357$), 50 μM (** $p = 0.0041$), and 100 μM (* $p = 0.0229$) (one-way ANOVA, ** $p = 0.0054$) (Figure 2B). TQ showed a significant inhibition in the CALR expression after 72 h at 20 μM (** $p = 0.0065$), 50 μM (** $p = 0.0033$), and 100 μM (** $p = 0.0029$) in a dose-dependent manner (one-way ANOVA, ** $p = 0.0016$) (Figure 2C). The expression levels were compared to those of the DMSO control, and each TQ concentration was performed in triplicate.

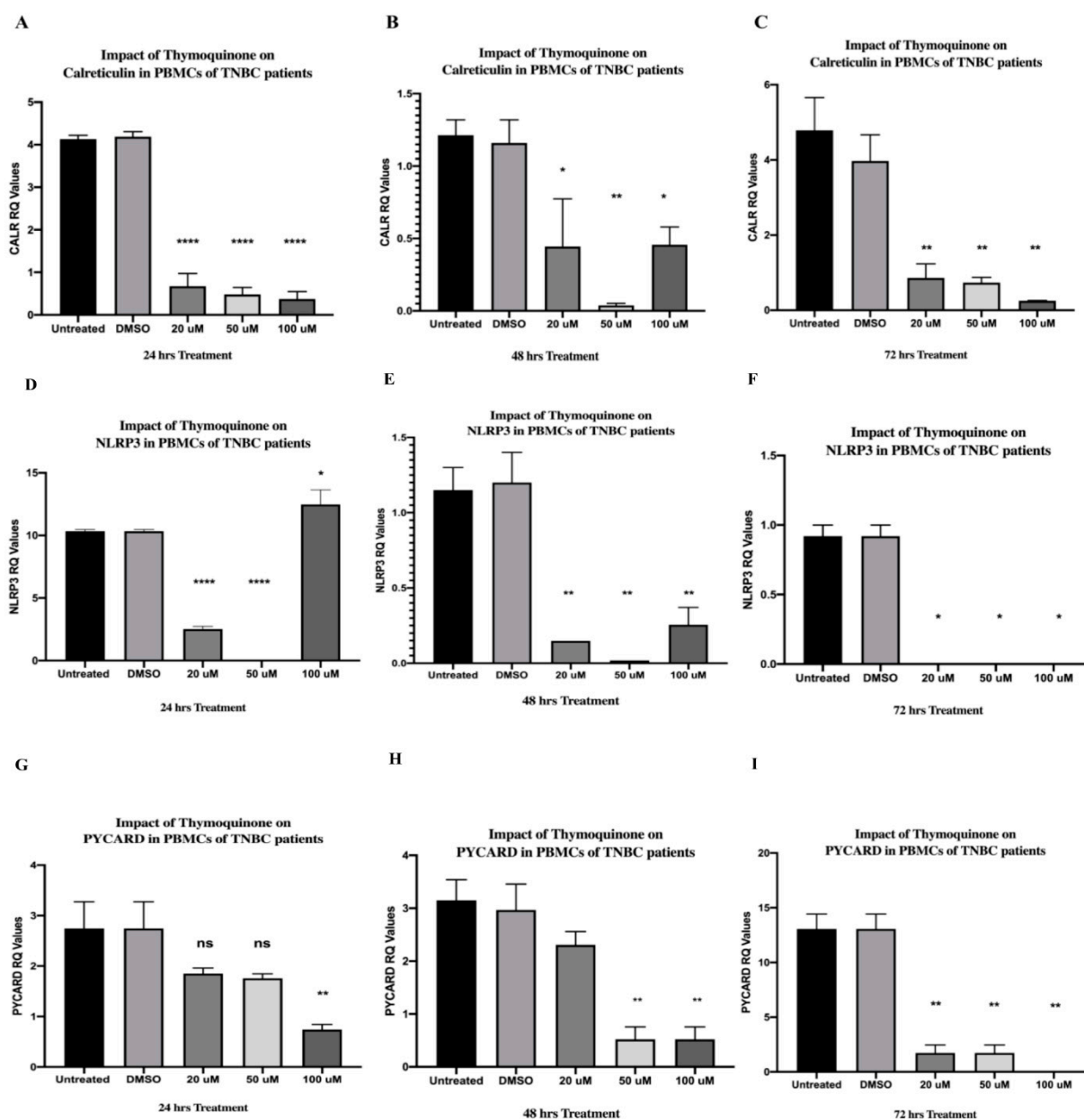


Figure 2. TQ significantly inhibited the expression of CALR, NLRP3 and PYCARD in PBMCs of TNBC patients. (A–C) CALR expression versus TQ concentrations. PBMCs isolated from TNBC patients were treated with TQ (0, 20, 50, and 100 μM) for (A) 24 h, (B) 48 h, and (C) 72 h. (D–F) NLRP3 expression versus TQ concentrations. PBMCs isolated from TNBC patients were treated with TQ (0, 20, 50, and 100 μM) for (D) 24 h, (E) 48 h, and (F) 72 h. (G–I) PYCARD expression versus TQ concentrations.

PBMCs isolated from TNBC patients were treated with TQ (0, 20, 50, and 100 μM) for (G) 24 h, (H) 48 h, and (I) 72 h. All experiments were performed in triplicate and data were expressed as the mean \pm standard deviation. Statistical analysis was performed using the GraphPad Prism software version 9.1.1. The data were analyzed using one-way ANOVA and Dunnett's multiple comparisons to compare each treated column and the DMSO control column (**** p value < 0.0001 ; ** p value < 0.01 ; * $p < 0.05$). TQ: thymoquinone; CALR: calreticulin; NLRP3: NOD-like receptor (NLR) family pyrin domain-containing protein 3 (NLRP3); PYCARD: PYD and CARD domain containing; PBMCs: peripheral blood mononuclear cells; TNBC: triple-negative breast cancer; BC: breast cancer; DMSO: dimethyl sulfoxide; ns: non-significant.

2.3. TQ Showed an Interesting Inhibitory Pattern in NLRP3 and PYCARD in PBMCs of HR+ BC Patients after 24 h of Treatment

The NLRP3 and PYCARD expressions were investigated with increasing TQ concentrations (20 μM , 50 μM , and 100 μM) after 24 h of treatment compared to those of the DMSO control, and each concentration was performed in triplicate. TQ caused a non-significant impact on NLRP3 expression at 20 μM ; then, a significant increase was noticed at 50 μM (**** $p < 0.0001$), followed by a complete abolishment in its expression at 100 μM (** $p = 0.0063$) (one-way ANOVA, **** $p < 0.0001$) (Figure 1D). TQ showed a similar inhibitory pattern in PYCARD expression after 24 h of treatment (Figure 1F). At first, it was significantly downregulated at 20 μM (** $p = 0.0059$), followed by a significant elevation at 50 μM (* $p = 0.0237$). Finally, its expression was significantly abolished below the detection level at 100 μM (*** $p = 0.0002$)—one-way ANOVA of PYCARD expression after 24 h of treatment: **** $p < 0.0001$.

2.4. TQ Inhibited NLRP3 and PYCARD Expressions in PBMCs of HR+ BC Patients after 48 and 72 h

TQ caused an initial non-significant increase in NLRP3 expression at 20 μM , followed by a significant downregulation at 50 μM (** $p = 0.0006$) and 100 μM (* $p = 0.0266$) after 48 h of treatment (one-way ANOVA, *** $p = 0.0006$) (Figure 1E). As for PYCARD, it showed a non-significant downregulation at 20 and 50 μM , followed by a significant increase at 100 μM (* $p = 0.0172$) after 48 h (one-way ANOVA, ** $p = 0.0010$) (Figure 1G). After 72 h of treatment, TQ caused a non-significant impact on PYCARD expression at 20 and 100 μM , whereas 50 μM significantly downregulated its expression (* $p = 0.0245$) (one-way ANOVA, $p = 0.0389$) (Figure 1H). The expression levels were compared to those of the DMSO control and each concentration was performed in triplicate.

2.5. TQ Strongly Inhibited NLRP3 Expression in PBMCs of TNBC Patients after 24 and 48 h of Treatment In Vitro and Completely Abolished Its Expression after 72 h

TQ showed a strongly significant inhibition in NLRP3 at 20 μM (**** $p < 0.0001$) followed by a completely abolished expression at 50 μM (**** $p < 0.0001$). Unexpectedly, TQ suddenly upregulated the NLRP3 expression at 100 μM (* $p = 0.0161$) after 24 h of treatment (one-way ANOVA **** $p < 0.0001$) (Figure 2D). After 48 h of TQ treatment, NLRP3 was significantly inhibited at 20 μM (** $p = 0.0050$), 50 μM (** $p = 0.0027$), and 100 μM (** $p = 0.0055$) (one-way ANOVA, ** $p = 0.0013$) (Figure 2E). The NLRP3 expression was completely inhibited after 72 h of TQ treatments at 20 μM (* $p = 0.0500$), 50 μM (* $p = 0.0500$), and 100 μM (* $p = 0.0500$) (one-way ANOVA, * $p = 0.0340$) (Figure 2F). Each TQ concentration was performed in triplicate and the expression levels were compared to those of the DMSO control.

2.6. TQ Significantly Inhibited PYCARD Expression in PBMCs Isolated from TNBC Patients after 24 and 48 h of Treatment

After 24 h of TQ treatment, the 20 μM and 50 μM concentrations resulted in a non-significant difference in PYCARD expression. In contrast, the 100 μM concentration significantly downregulated its expression (** $p = 0.0070$) (one-way ANOVA, * $p = 0.0108$) (Figure 2G). PBMCs were further incubated for 48 h and showed a significant inhibition in

PYCARD expression at 50 μM (** $p = 0.0068$) and 100 μM (** $p = 0.0068$), while the 20 μM concentration caused a non-significant inhibition (one-way ANOVA, ** $p = 0.0044$) (Figure 2H). TQ significantly inhibited the expression of PYCARD at 20 μM (** $p = 0.0052$) and 50 μM (** $p = 0.0052$) and completely abolished its expression after 72 h at 100 μM (** $p = 0.0065$) (one-way ANOVA, ** $p = 0.0027$) (Figure 2I). TQ concentrations were performed in triplicate and the expression levels were compared to those of the DMSO control.

2.7. TQ Significantly Inhibited Caspase-1 after 24, 48, and 72 h of Treatment in PBMCs of HR+ BC Patients

After 24 h of treating PBMCs isolated from HR+ BC patients with 20 μM TQ, an initial non-significant upregulation was observed in caspase-1, followed by a significant dampening in its expression at 50 μM (* $p = 0.0195$); finally, it was significantly upregulated at 100 μM (** $p = 0.0013$) (one-way ANOVA, *** $p = 0.0002$) (Figure 3A). After 48 h, TQ significantly inhibited caspase-1 expression in a dose-dependent manner with increasing TQ concentrations (50 and 100 μM) (**** $p < 0.0001$), whereas 20 μM caused a non-significant downregulation (one-way ANOVA, **** $p < 0.0001$) (Figure 3B). After 72 h of treatment, TQ showed a strongly significant downregulation of caspase-1 expression at 20, 50, and 100 μM (**** $p < 0.0001$) (one-way ANOVA, **** $p < 0.0001$) (Figure 3C). The expression levels were compared to those of the DMSO control and each concentration was performed in triplicate.

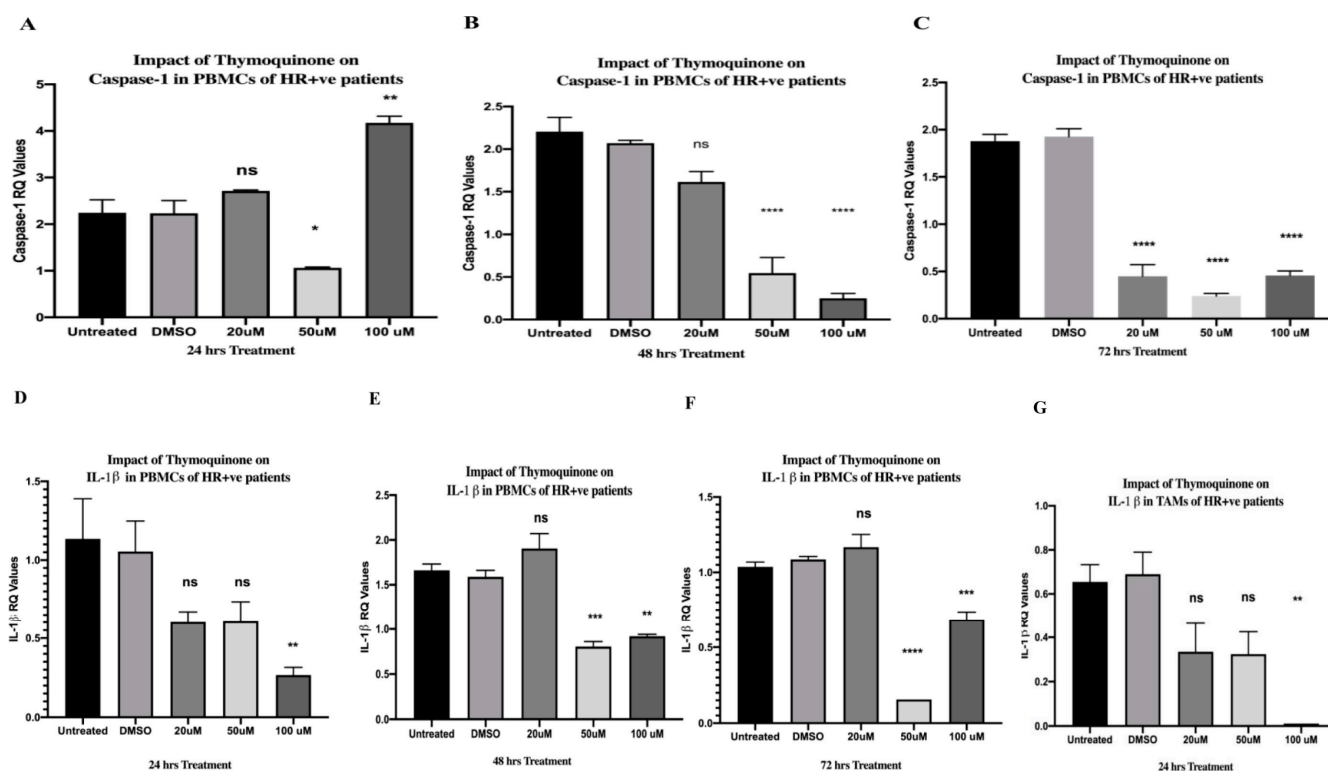


Figure 3. Inhibitory impact of TQ on caspase-1 and IL-1 β expression in PBMCs and TAMs of HR+ BC patients, respectively. (A–C) Caspase-1 expression versus TQ concentrations. PBMCs isolated from HR+ BC patients were treated with TQ (0, 20, 50, and 100 μM) for (A) 24 h, (B) 48 h, and (C) 72 h. (D–F) IL-1 β expression versus TQ concentrations. PBMCs isolated from HR+ BC patients were treated with TQ (0, 20, 50, and 100 μM) for (D) 24 h, (E) 48 h, and (F) 72 h. (G) Impact of TQ on IL-1 β expression in TAMs isolated from HR+ BC patients after 24 h. All experiments were performed in triplicate and data are expressed as the mean \pm standard deviation. Statistical analysis was performed using the GraphPad Prism software version 9.1.1. The data were analyzed using one-way ANOVA and Dunnett’s multiple comparisons to compare each treated column and the DMSO control column (**** p value < 0.0001 ; *** p value < 0.001 ; ** p value < 0.01 ; * p < 0.05).

TQ: thymoquinone; HR+: hormone receptor-positive; BC: breast cancer; ns: non-significant; IL-1 β : Interleukin-1 beta; PBMCs: peripheral blood mononuclear cells; TAMs: tumor-associated macrophages.

2.8. TQ Showed a Dose-Dependent Inhibitory Effect on Caspase-1 Expression in PBMCs Isolated from TNBC In Vitro

TQ showed a non-significant downregulation in caspase-1 expression at 20 μ M, while TQ significantly dampened its expression at 50 μ M (** $p = 0.0065$) and 100 μ M (***) $p = 0.0006$) TQ concentrations after 24 h of treatment in vitro (one-way ANOVA, *** $p = 0.0003$) (Figure 4A). After 48 h of TQ treatments, caspase-1 expressions were significantly inhibited at 20 μ M (* $p = 0.0164$), 50 μ M (** $p = 0.0015$), and 100 μ M (* $p = 0.0254$) (one-way ANOVA, *** $p = 0.0010$) (Figure 4B). PBMCs were further incubated for 72 h with the aforementioned TQ concentrations. Results showed non-significant differences in caspase-1 expression at 20 μ M and 50 μ M, whereas the 100 μ M concentration significantly inhibited its expression (** $p = 0.0013$) (one-way ANOVA, ** $p = 0.0014$) (Figure 4C). TQ concentrations were performed in triplicate and the expression levels were compared to those of the DMSO control.

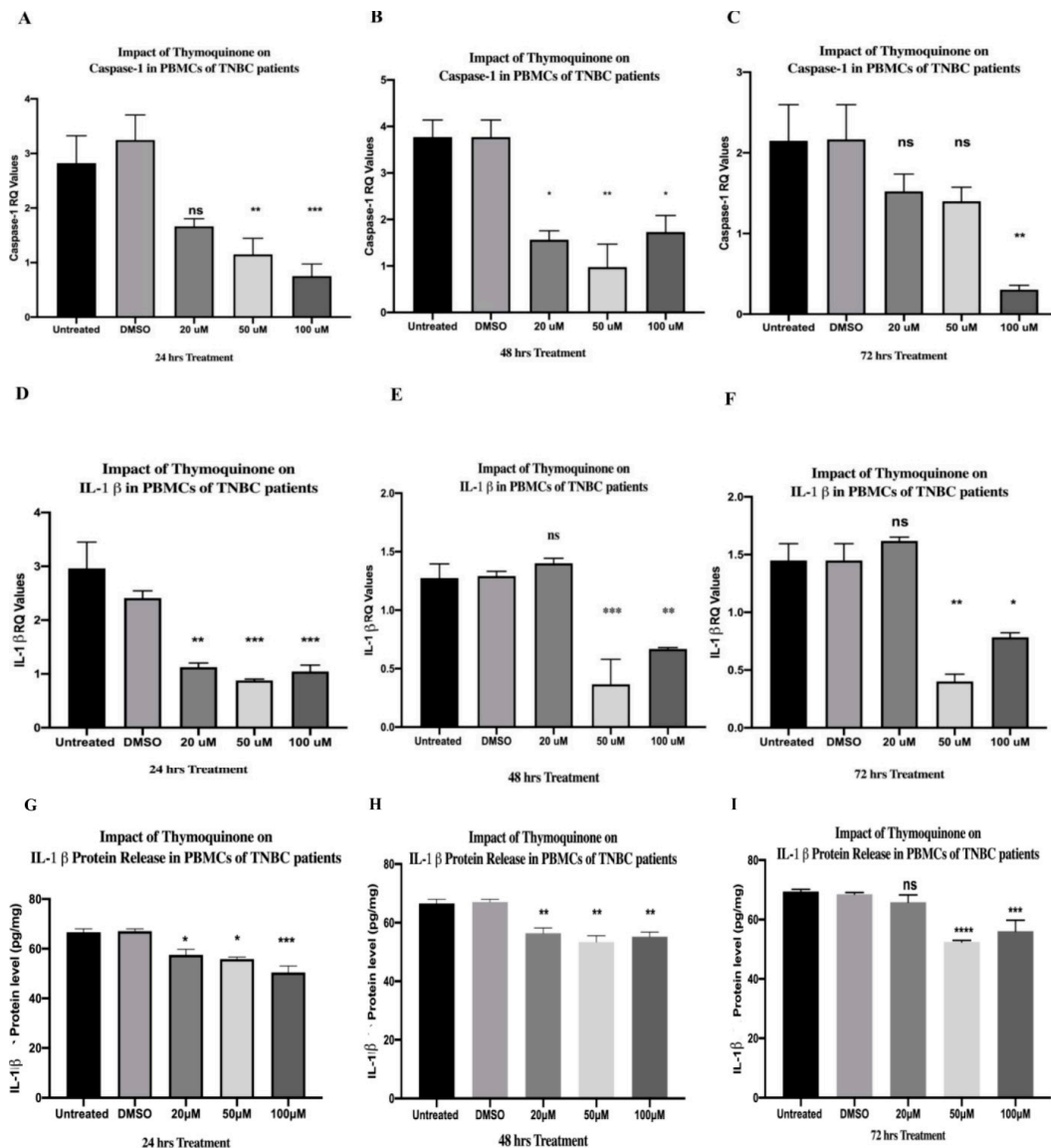


Figure 4. TQ inhibited caspase-1 expression, IL-1 β expression, and protein release in PBMCs of TNBC patients. (A–C) Caspase-1 expression versus TQ concentrations. PBMCs isolated from TNBC

patients were treated with TQ (0, 20, 50, and 100 μM) for (A) 24 h, (B) 48 h, and (C) 72 h. (D–F) IL-1 β expression versus TQ concentrations. PBMCs isolated from TNBC patients were treated with TQ (0, 20, 50, and 100 μM) for (D) 24 h, (E) 48 h, and (F) 72 h. (G–I) IL-1 β protein levels (pg/mL) secreted from PBMCs of TNBC patients treated with TQ concentrations (0, 20, 50, and 100 μM) for (G) 24 h, (H) 48 h, and (I) 72 h. All experiments were performed in triplicate, and data were expressed as the mean \pm standard deviation. Statistical analysis was performed using the GraphPad Prism software version 9.1.1. The data were analyzed using one-way ANOVA and Dunnett's multiple comparisons to compare each treated column and the DMSO control column (**** p value < 0.0001; *** p value < 0.001; ** p value < 0.01; * p < 0.05). TQ: thymoquinone; TNBC: triple-negative breast cancer; BC: breast cancer; ns: non-significant; IL-1 β : Interleukin-1 beta; PBMCs: peripheral blood mononuclear cells; DMSO: dimethyl sulfoxide.

2.9. TQ Significantly Downregulated IL-1 β Expression in a Dose-Dependent Manner in PBMCs of HR+ BC Patients

After 24 h, TQ caused a non-significant difference at 20 μM or 50 μM . Interestingly, TQ significantly inhibited IL-1 β at 100 μM (** p = 0.0012) (one-way ANOVA, ** p = 0.0011) (Figure 3D). Since TQ showed an inhibitory effect on IL-1 β , the current study investigated longer treatment durations. Similarly, TQ significantly downregulated the expression of IL-1 β at 50 μM and 100 μM after 48 h (*** p = 0.0008 and ** p = 0.0017, respectively). TQ strongly inhibited the expression of IL-1 β after 72 h at 50 μM (**** p < 0.0001) and 100 μM (** p = 0.0002), whereas the 20 μM concentration caused a non-significant change—one-way ANOVA of IL-1 β expression after 48 and 72 h of treatment, **** p < 0.0001 (Figure 3E,F). The expression levels were compared to those of the DMSO control and each concentration was performed in triplicate.

2.10. TQ Significantly Downregulated IL-1 β Expression in PBMCs of TNBCs

TQ significantly downregulated the expression of IL-1 β at 20 μM (** p = 0.0020), 50 μM (*** p = 0.0010), and 100 μM (*** p = 0.0007) after 24 h of treatment (one-way ANOVA, *** p = 0.0007) (Figure 4D). PBMCs were further incubated for 48 and 72 h. Results showed a non-significant upregulation in IL-1 β at 20 μM after 48 h, while the 50 μM (*** p = 0.0005) and 100 μM (** p = 0.0071) concentrations significantly inhibited its expression (one-way ANOVA, *** p = 0.0001) (Figure 4E). TQ treatment for 72 h showed similar findings; there was a non-significant upregulation in IL-1 β at 20 μM , while the 50 μM (** p = 0.0013) and 100 μM (* p = 0.0123) concentrations significantly inhibited its expression (one-way ANOVA of IL-1 β , *** p = 0.0007) (Figure 4F). TQ concentrations were performed in triplicate and the expression levels were compared to those of the DMSO control.

2.11. Microscopic and Flow Cytometry Results of Efficient CD14+ Monocyte Differentiation to Tumor-Associated Macrophages (TAMs)

To validate that the cultured CD14+ monocytes were successfully differentiated to TAMs, microscopic examination and flow cytometry (CD163 positivity) were performed to compare monocytes to TAMs. Microscopic examination revealed morphological changes. The freshly isolated monocytes showed cells that were small in size with a spherical and smooth surface (Figure 5A). On day 7, cells showed TAMs morphology, which was larger in size relative to that of monocytes and had edgy and rough surfaces, showing efficient TAMs differentiation (Figure 5B).

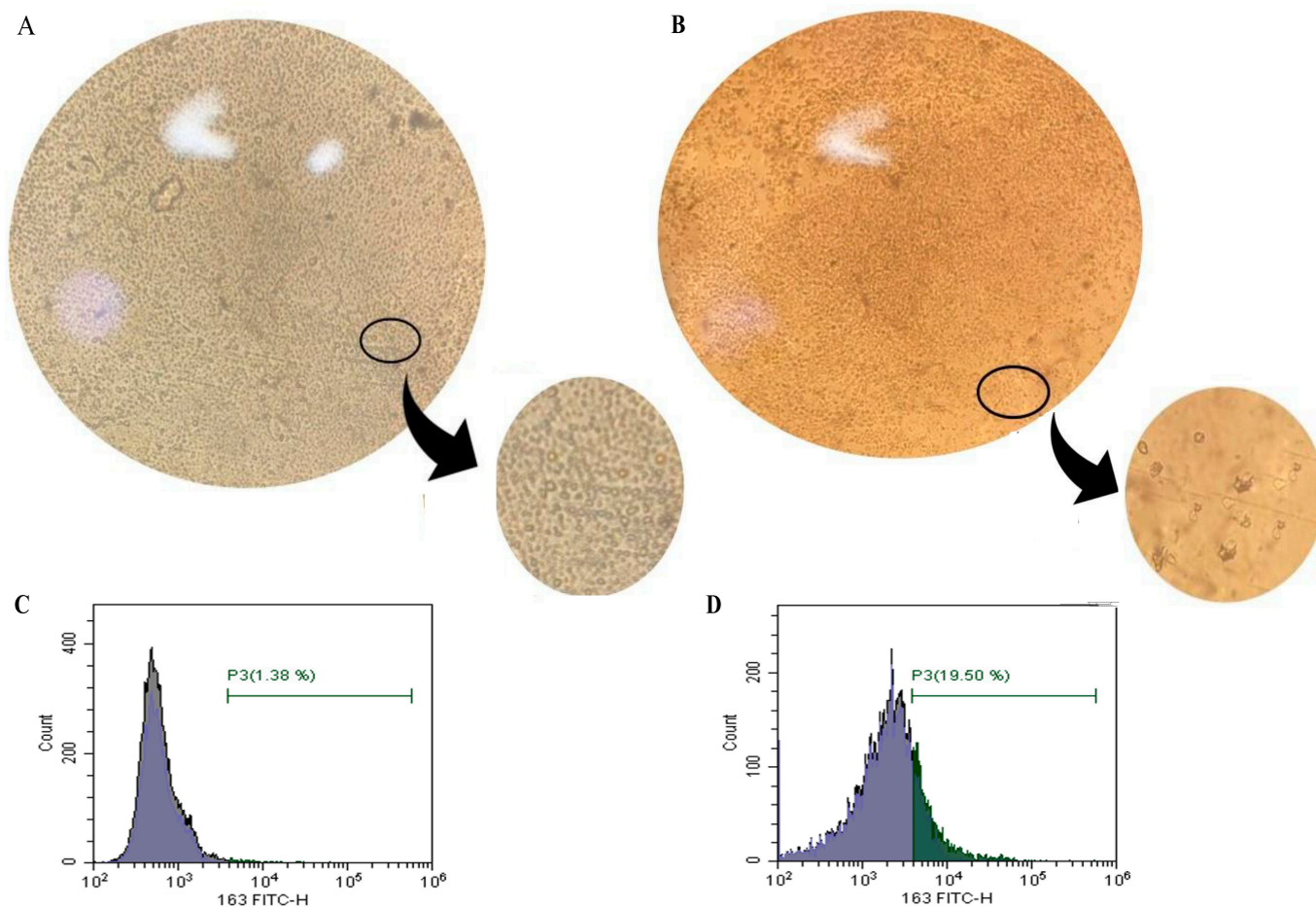


Figure 5. Efficiency of CD14+ monocyte differentiation to tumor-associated macrophages (TAMs). (A,B) Microscopic examination. (A) The figure shows freshly isolated and undifferentiated CD14+ monocytes characterized by relatively small size, with a spherical and smooth surface. (B) Differentiated TAMs morphology was observed on day 7 after culturing monocytes with culture media, tumor-conditioned media, IL-10, IL-4, and MCSF. Examination showed morphological changes; cells became relatively larger in size with edge and rough surfaces confirming TAMs differentiation. (C,D) Flow cytometric analysis utilizing anti-CD163 FITC. (C) Freshly isolated undifferentiated CD14+ monocytes showed low CD163 positivity (1.38%). (D) After seven days of culturing monocytes with culture media, tumor-conditioned media, IL-10, IL-4, and MCSF, flow cytometry showed a 14-fold increase in CD163 positivity (19.50%) compared to that of undifferentiated CD14+ monocytes confirming efficient TAMs differentiation. TAMs: tumor-associated macrophages; BC: breast cancer; IL-10: interleukin-10; IL-4: interleukin-4; MCSF: macrophage-colony stimulating factor.

To further confirm efficient TAMs differentiation and since CD163 is a TAMs biomarker [108], flow cytometry was performed to test the increase in CD163 positivity in TAMs relative to that of undifferentiated monocytes. Upon staining with anti-CD163, results showed that TAMs CD163 positivity increased and was even 14-fold higher than that of freshly isolated monocytes (19.5% CD163-positive versus 1.38%, respectively). Thus, TAMs morphology and increased CD163 positivity confirmed successful TAMs differentiation (Figure 5C,D).

2.12. TQ Significantly Abolished the Expression of IL-1 β in TAMs Isolated from HR+ BC Patients

TAMs are a major source of high IL-1 β secretion [73,74], which causes a significant decrease in ER α levels [76], endocrine- and chemo-resistance in HR+ BC [75–77]. The impact of TQ on the expression of IL-1 β , specifically in TAMs, was further investigated. TQ significantly abolished the expression of IL-1 β in TAMs after treatment for 24 h at 100 μ M

(** $p = 0.0014$)—one-way ANOVA, ** $p = 0.0018$ (Figure 3G). The expression levels were compared to those of the DMSO control and each concentration was performed in triplicate.

Using ELISA, the current study further investigated the TQ's impact on IL-1 β protein release in PBMCs of HR+ BC patients and TAMs.

2.13. TQ Significantly Downregulated Protein Release of IL-1 β in PBMCs and TAMs of HR+ BC Patients

After 24 h of TQ treatment, the 20 μM concentration caused a non-significant downregulation in the protein release of IL-1 β , followed by a significant decrease at 50 μM (** $p = 0.0025$) and 100 μM (* $p = 0.0102$)—one-way ANOVA, *** $p = 0.0009$ (Figure 6A). TQ caused a non-significant downregulation, followed by a significant decrease at 50 μM (**** $p < 0.0001$) and 100 μM (*** $p = 0.0008$) after 48 h of treatment (one-way ANOVA, **** $p < 0.0001$) (Figure 6B). After 72 h of treatment, TQ significantly lessened the protein release of IL-1 β at 20 μM (** $p = 0.0046$), 50 μM (** $p = 0.0035$), and 100 μM (*** $p = 0.0008$)—one-way ANOVA, *** $p = 0.0002$ (Figure 6C). The impact of TQ on the protein release of IL-1 β was further investigated in TAMs of HR+ BC patients. A concentration of 20 and 50 μM of TQ showed a non-significant impact on IL-1 β release. However, the 100 μM concentration significantly downregulated IL-1 β protein release (* $p = 0.0390$)—one-way ANOVA, ** $p = 0.0080$ (Figure 6D). The protein levels were compared to those of the DMSO control, and each TQ concentration was performed in triplicate.

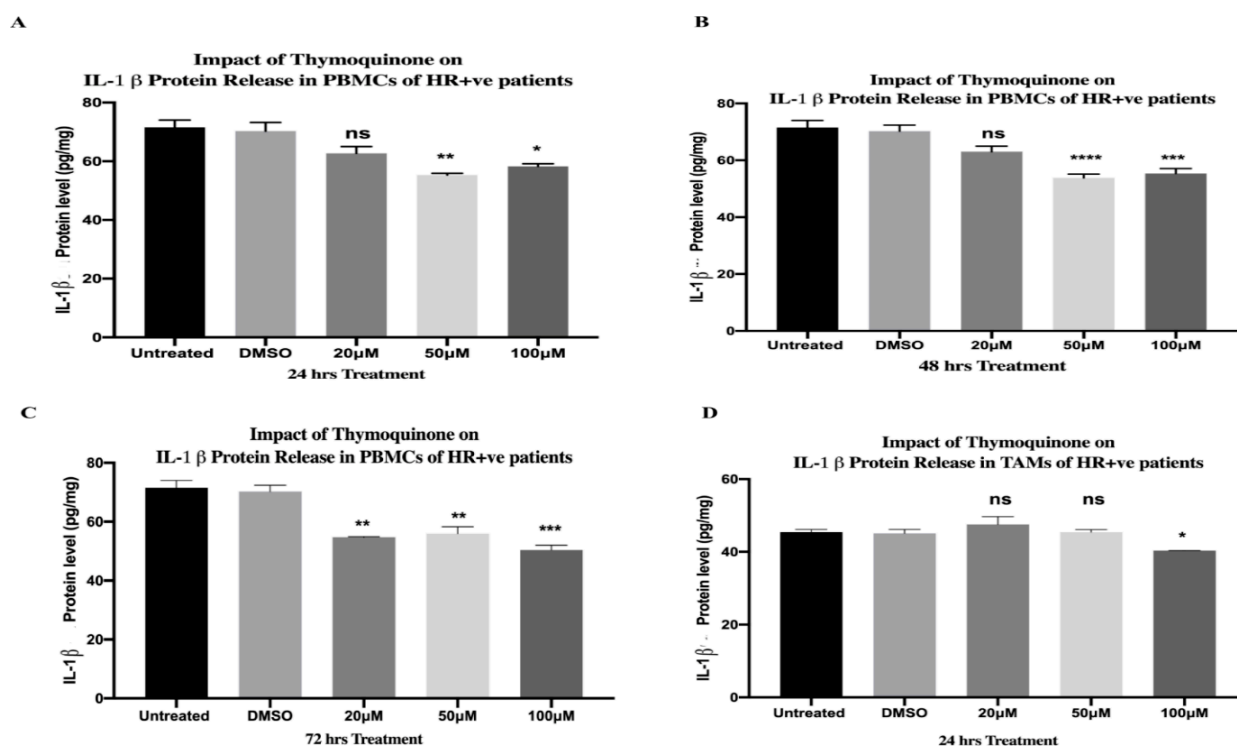


Figure 6. TQ significantly inhibited the protein release of IL-1 β in PBMCs and TAMs of HR+ BC, respectively. (A–C) IL-1 β protein level (pg/mL) released from PBMCs of HR+ BC patients treated with TQ concentrations (0, 20, 50, and 100 μM) for (A) 24 h, (B) 48 h, and (C) 72 h. (D) IL-1 β protein level (pg/mL) released from TAMs of HR+ BC patients treated with TQ concentrations (0, 20, 50, and 100 μM) for 24 h. All experiments were performed in triplicate and data were expressed as the mean \pm standard deviation. Statistical analysis was performed using the GraphPad Prism software version 9.1.1. The data were analyzed using one-way ANOVA and Dunnett's multiple comparisons to compare each treated column and the DMSO control column (**** p value < 0.0001 ; *** p value < 0.001 ; ** p value < 0.01 ; * $p < 0.05$). TQ: thymoquinone; ns: non-significant; DMSO: dimethyl sulfoxide; PBMCs: peripheral blood mononuclear cells; TAMs: tumor-associated macrophages, HR+: hormone receptor-positive; BC: breast cancer; IL-1 β : interleukin-1 beta.

2.14. TQ Significantly Downregulated IL-1 β Protein Release from PBMCs of TNBC Patients

TQ significantly downregulated the protein release of IL-1 β after 24 h at 20 μ M (* $p = 0.0296$), 50 μ M (* $p = 0.0134$), and 100 μ M (*** $p = 0.008$)—one-way ANOVA, ** $p = 0.0013$ (Figure 4G). Similarly, 20 μ M (** $p = 0.0067$), 50 μ M (** $p = 0.0015$), and 100 μ M (** $p = 0.0012$) of TQ treatments significantly downregulated its protein release after 48 h (one-way ANOVA, *** $p = 0.0007$) (Figure 4H). After 72 h, 20 μ M TQ did not cause a significant change in IL-1 β protein release, while the 50 μ M (**** $p < 0.0001$) and 100 μ M (*** $p = 0.005$) concentrations significantly downregulated its release (one-way ANOVA, (**** $p < 0.0001$). (Figure 4I). TQ concentrations were performed in triplicate and the protein levels were compared to those of the DMSO control.

2.15. PBMCs of TNBC Patients Released Significantly Higher sPD-L1 Than That of HR+ BC Patients

The current study compared the release of sPD-L1 from PBMCs of TNBC patients in DMSO control and that of luminal A HR+ via ELISA. Results showed that PBMCs of TNBC patients released significantly higher protein levels of sPD-L1 than those of luminal A HR+ BC patients (**** $p < 0.0001$). Data were analyzed using an unpaired t -test (Figure 7A). Thus, the present study investigated the impact of increasing TQ concentrations for various durations on sPD-L1 in TNBC only.

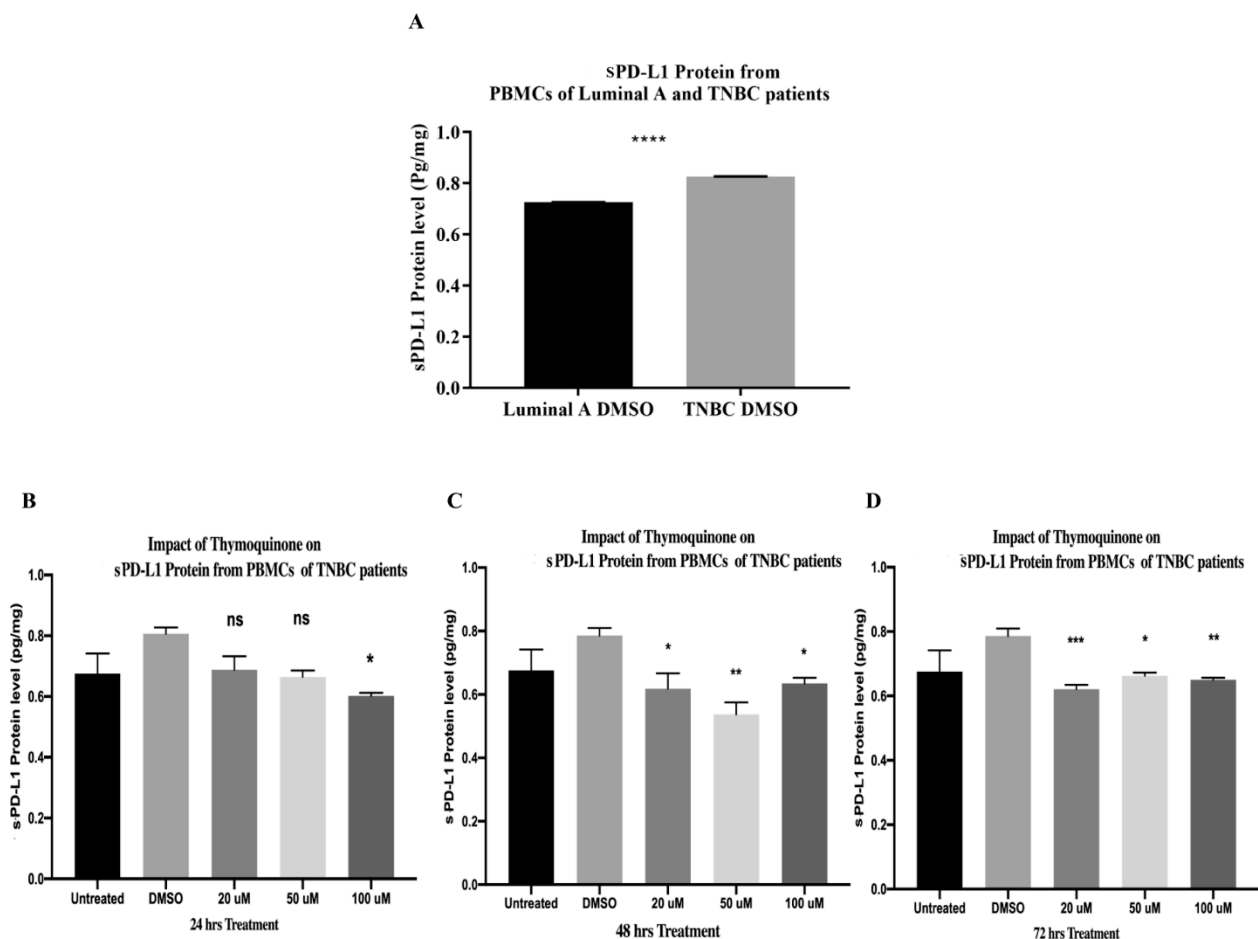


Figure 7. (A) sPD-L1 release in HR+ luminal A and TNBC patients. (A) sPD-L1 protein level (pg/mL) released from PBMCs of HR+ BC luminal A and TNBC patients in DMSO control. sPD-L1 from PBMCs of TNBC patients was significantly higher than that of luminal A HR+ BC patients (**** $p < 0.0001$). Data were analyzed using unpaired t -test. (B–D) TQ significantly inhibited sPD-L1 release from PBMCs of TNBC patients. ELISA quantified sPD-L1 protein level (pg/mL) released from PBMCs of TNBC patients treated with TQ concentrations (0, 20, 50, and 100 μ M) for (B) 24 h,

(C) 48 h, and (D) 72 h. All experiments were performed in triplicate and data were expressed as the mean \pm standard deviation. Statistical analysis was performed using the GraphPad Prism software version 9.1.1. The data were analyzed using one-way ANOVA and Dunnett's multiple comparisons to compare each treated column and the DMSO control column (**** p value < 0.0001 ; *** p value < 0.001 ; ** p value < 0.01 ; * p < 0.05). TQ: thymoquinone, HR+: Hormone receptor-positive; TNBC: triple-negative breast cancer; BC: breast cancer; ns: non-significant; sPD-L1: soluble programmed death ligand 1; PBMCs: peripheral blood mononuclear cells; DMSO: dimethyl sulfoxide; ELISA: enzyme-linked immunosorbent assay.

2.16. TQ Significantly Downregulated sPD-L1 Release from PBMCs of TNBC Patients after 24, 48, and 72 h of Treatment In Vitro

After 24 h of treatment, TQ showed a non-significant impact on sPD-L1 from PBMCs of TNBC patients at 20 μ M and 50 μ M. However, 100 μ M significantly downregulated its protein level (* p = 0.0468) (Figure 7B). After 48 h of TQ treatments, 20 μ M (* p = 0.0435), 50 μ M (** p = 0.0014), and 100 μ M (* p = 0.0300) significantly downregulated sPD-L1 release (one-way ANOVA, p = 0.0066) (Figure 7C). After 72 h of treatment, TQ caused a significant downregulation in sPD-L1 protein release at 20 μ M (** p = 0.0008), 50 μ M (* p = 0.0101), and 100 μ M (** p = 0.0047)—one-way ANOVA, p = 0.0037 (Figure 7D). TQ concentrations were performed in triplicate and the protein levels were compared to those of the DMSO control.

3. Discussion

More than approximately 60% of the available anticancer drugs were derived from natural sources, in one way or another [109]. Plant-derived agents such as vincristine and paclitaxel are among the most effective cancer chemotherapeutics [110]. Interestingly, various chemotherapeutics led to the secretion of danger signals [111] such as CALR [16] which showed various tumor-promoting effects in BC and has been recently addressed as a biological marker of BC [28–34]. CALR has been reported to be an activator to the NLRP3 pathway [36–39]. In BC, NLRP3 and PYCARD expressions were strongly associated with pro-tumorigenic and aggressive clinicopathological features in luminal [61] and TNBC patients [62]. NLRP3 activation promoted immune system dysfunction [64], BC growth, enhanced angiogenesis [63], migration [112], and BC metastasis [63,64]. The downstream IL-1 β was correlated with large tumor size, clinical stage, histological grade [70,72], endocrine- and chemo-resistance in HR+ BC patients [75–77]. Moreover, IL-1 β production by peripheral blood cells enhanced lymphatic metastasis in BC [69]. Recently, sPD-L1 has attracted much attention [85] since its high serum levels were correlated with metastasis, immunosuppression, and poor prognosis in TNBC patients [87,88]. Interestingly, IL-1 β induced sPD-L1 release [86]. Elevated IL-1 β and sPD-L1 levels showed a significantly shorter progression-free survival in BC patients [89], highlighting the beneficial impacts of targeting IL-1 β in both HR+ and TNBC patients. It has been shown that BC is a systemic inflammatory disease [3–5], where peripheral blood represents reservoirs and activation sites of immune cells during BC progression [6]. CALR [22–26], NLRP3 [45–51], and IL-1 β [65–68] have been shown to be expressed in PBMCs and were addressed as markers of systemic inflammation [52,113,114], as well as sPD-L1 that was recently indicated as a sign of inflammation [86]. The current study aimed to target the aforesaid pro-tumorigenic BC markers comprising CALR, NLRP3 complex, sPD-L1, and IL-1 β in PBMCs and TAMs of TNBC and HR+ BC patients, respectively. NLRP3 required two signals for activation: the first one was the priming step that needed the transcription of NLRP3 components and pro-IL-1 β via NF- κ B [115,116], while the second signal was through various danger signals that led to the oligomerization of inflammasome components and the formation of an NLRP3-active complex, and then, finally, the secretion of IL-1 β [115–117]. For the first time, the present study explored the inhibitory impact of TQ on the aforementioned components since it suppressed NF- κ B activation in BC [118] and dampened NLRP3 in human and mouse melanoma in vitro [101]. In addition, a recent study discussed the inhibitory impact of TQ on PD-L1 in the TNBC cell line [107].

CALR resides in the ER, acting as a chaperone in healthy cells [17]. When cells are exposed to stress/injury such as chemotherapy [18], radiation [19], and oncolytic peptides [20], CALR translocates to the cell surface, acting as a DAMP [21,119]. The translocated CALR can be released into the extracellular milieu [27]. Recently, CALR has been addressed as a novel biological BC marker and an indicator of BC staging and prognosis [28–32]. Moreover, CALR expression was associated with more advanced BC tumors [33] and mediated invasive BC phenotype [34]. In addition, it was correlated with enhanced metastasis in BC patients [31]. Notably, ER contains other chaperones that assist in protein folding processes, such as glucose-regulated protein GRP78 [120]. Like in the case of CALR, stressful conditions upregulated GRP78's translocation on the surface of the cell membrane [121], and it was elevated in endocrine-resistant BC that directly affected the responsiveness to anti-estrogen therapy [122]. In TNBC, GRP78 has been shown to interact with PD-L1 at the ER region and increase its levels [123]. The current study showed that TQ was a successful inhibitor of CALR expression in PBMCs of HR+ and TNBC patients in various concentrations and durations, as shown in Figure 8A. Although this is the first study to report the inhibitory effect of TQ on CALR in general and specifically in BC, the literature reported that TQ inhibited the expression of GRP78 in a rat model in vivo [124]. A study in multiple myeloma showed that high CALR expression was associated with an increased PD-L1 level [125]. Another study noticed that doxorubicin enhanced CALR and PD-L1 expression in BC cells in a dose-dependent manner [126], highlighting the potential role of CALR in immunosuppression and resistance. Interestingly, a recent study elaborated that tumors release a soluble CALR [127] that acts as a decoy for CALR receptors in phagocytes inhibiting the uptake of dying cancer cells leading to the accumulation of immunosuppressive cells in peripheral blood [128], immune evasion [129], and resistance to PD-1/PD-L1 blockade [127]. This raises a number of questions that require urgent investigation: Does soluble CALR interact with sPD-L1 aggravating immunosuppression? Does CALR interact with PD-L1 in the ER, causing immunotherapy resistance in BC? Also, it would be worth further examining the effect of TQ on CALR/PD-L1 and GRP78/PD-L1 expression in TNBC patients in vivo.

Various studies demonstrated that CALR is an NLRP3 activator [36–39]. The inhibitory impact of TQ on NLRP3 in BC was not investigated to date. It has been noticed that the most common concentrations of TQ in various BC cell lines ranged from 20 to 100 μM [118,130–134] and were commonly incubated for 24, 48, and 72 h [93,98,130,135–137]. In addition, a recent study showed that TQ was not cytotoxic to PBMCs at concentrations of 100, 50, 25, 12.5, 6.25, 3.125, 1, and 0.1 μM (medium containing $\leq 0.1\%$ DMSO) incubated for 24, 48, and 72 h [99]. Interestingly, TQ has even been shown to proliferate PBMCs [99]. Another study stated that 50 and 100 μM TQ concentrations enhanced monocyte-derived macrophage activity and noticed an increase in the phagocytotic abilities after the TQ treatment [100]. Thus, 20, 50, and 100 μM TQ concentrations incubated for the aforementioned durations were chosen in this study. NLRP3 expression was significantly inhibited dose-dependently by TQ in PBMCs of HR+ BC patients and TNBC patients, as summarized in Figure 8A. The aforementioned results came in accordance with those for A375 and B16F10 melanoma cells [101], where 5–20 μM of TQ significantly decreased NLRP3 expression in a dose-dependent manner [101]. In view of the fact that TNBC and HR+ subtypes are immunohistochemically distinct [138–142], it has been noticed that after 24 h of TQ treatment, 50 μM TQ upregulated NLRP3 followed by a completely abolished expression at 100 μM in PBMCs of HR+ BC (Figure 1D). On the contrary, in PBMCs of TNBC, 50 μM abolished its expression, followed by significant upregulation at 100 μM after 24 h of TQ treatment (Figure 2D). This demonstrates that TQ's inhibitory concentrations differ from one BC subtype to another. As for PYCARD expression, TQ significantly downregulated its expression in PBMCs of HR+ and TNBC patients (Figure 8A). This came in accordance with an in vivo study where TQ significantly downregulated the PYCARD expression in rats fed with ethanol and a high-fat diet [102]. Notably, 50 μM and 100 μM TQ incubated for 24 h (Figure 1F) showed a similar pattern to that of the NLRP3 expression in HR+ PBMCs

(Figure 1D), where it significantly upregulated the PYCARD expression at 50 μM , followed by a completely abolished PYCARD expression at 100 μM (Figure 1F).

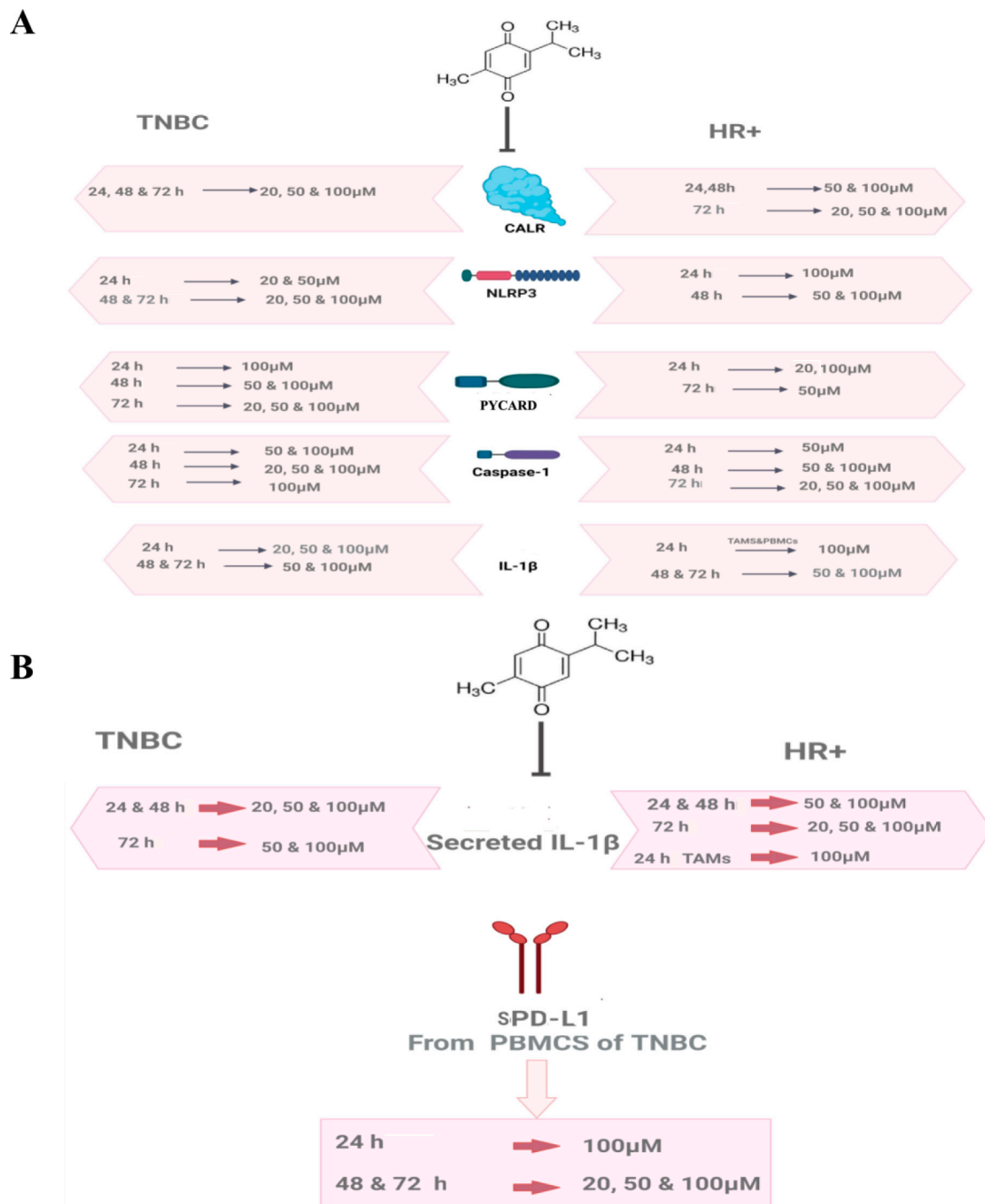


Figure 8. Summary of TQ's significant inhibitory concentrations for distinct durations on CALR, inflammasome pathway, and sPD-L1 in HR+ and TNBC. (A) TQ's significant inhibitory concentrations on expression of CALR, NLRP3 complex components and IL-1 β in PBMCs/TAMs of HR+ and TNBC after 24, 48, and 72 h of treatment. (B) The significant inhibitory concentrations of TQ after 24, 48, and 72 h of treatment on IL-1 β and sPD-L1 secretion from TAMs/PBMCs of HR+ and TNBC, respectively. The expression and protein levels were compared to those of the DMSO control. All experiments were performed in triplicate. TQ: thymoquinone; CALR: calreticulin; NLRP3: NOD-like receptor (NLR) family pyrin domain-containing protein 3 (NLRP3); PYCARD: PYD and CARD domain containing; PBMCs: peripheral blood mononuclear cells; TAMs: tumor-associated macrophages; HR+: hormone receptor-positive; TNBC: triple-negative breast cancer; BC: breast cancer; DMSO: dimethyl sulfoxide; IL-1 β : interleukin-1 beta; sPD-L1: soluble programmed death ligand 1.

Caspase-1 is an inflammatory caspase that is activated via inflammasome complexes in response to DAMPs or pathogen-associated molecular patterns (PAMPs) [143]. Since it is a protease, it cleaves the proinflammatory cytokine IL-1 β into its active form after its activation [143]. TQ significantly inhibited caspase-1 expression in PBMCs of HR+ and TNBC (Figure 8A), which came in accordance with distinct *in vivo* and *in vitro* studies [101,103,104]. In BC, high levels of IL-1 β showed various tumor-promoting impacts [144–146]. Peripheral blood cells of invasive BC patients produced high levels of IL-1 β , leading to metastasis [69]. In sera and plasma of BC patients, ELISA findings showed that IL- β expressions were significantly increased compared to those in the control group [70,71]. Remarkably, IL-1 β is secreted via not only the inflammasome pathway [143], but also NF- κ B [115,116] which is activated via extracellular ATP [147] and the purinergic receptor P2X7R [148]. The released IL-1 β was found to promote the production of pro-IL-1 β by binding to the IL-1 receptor, which is expressed in various BC cells, including MDA-MB231 [149]. TAMs are a major source of IL-1 β expression and secretion [73,74] and important BC promoters [150]. HR+ BC patients exhibited high levels of IL-1 β leading to metastasis [77], downregulation of ER α [76], chemo-resistance, and endocrine resistance [77], which has been shown to be a great challenge in the treatment of hormonal BC patients [151]. In addition, IL-1 β provoked progression in TNBC and its inhibition showed synergistic impacts in combination with a PD-L1 blocker [152]. Thus, in the current study, there was a focus on IL-1 β in PBMCs and TAMs of TNBC and HR+ BC patients, respectively. Because IL-1 β is secreted via various pathways, TQ as an inhibitor to NF κ B [118] and NLRP3 in melanoma [101] was an excellent candidate to lessen its expression in the current study. Moreover, the literature demonstrated that patients with BC might experience a change in their BC subtype after neoadjuvant chemotherapy (nCT), leading to a change in adjuvant treatment in 100% of such patients [153]. That is why the HER2 and HR status, including the ER and the progesterone receptor (PR), should be evaluated not only before the initiation of nCT, but also after nCT [153]. Since IL-1 β contributed to a significant decrease in ER α levels [76], further studies should be conducted to unravel the hidden reasons for such BC subtype conversion after nCT and clarify whether inflammasome pathway and the subsequent IL-1 β secretion are responsible for such change. The current study showed that TQ significantly inhibited IL-1 β expression and protein release in TAMs and PBMCs isolated from HR+ and TNBC patients, respectively (Figure 8A,B). The aforementioned inhibitory impacts on IL-1 β came in accordance with distinct *in vivo* and *in vitro* studies [101–105,154].

To date, the current study is the only available investigation of TQ's impact on NLRP3 in BC. However, various research articles examined its inhibitory effect on NLRP3 in various models [101–106]. One study examined its inhibitory impact on NLRP3 in human and mouse melanoma *in vitro* with increasing concentrations of TQ: 5, 10, and 20 μ M for a fixed duration (24 h); TQ showed a dose-dependent inhibitory effect [101]. In the pancreatitis model, rats were treated with 100 mg/kg orally [102] and an oral TQ dose of 50 mg/kg/day in acute kidney injury [103] and cardiac damage in mice models *in vivo* [104,105]. In the Alzheimer's rat model, oral administration of 10 mg/kg TQ ameliorated neuroinflammation via suppressing mRNA and protein levels of NLRP3 and IL-1 β [106]. Interestingly, TQ significantly inhibited the expression of NLRP3 and its downstream proteins in all *in vivo* models [102–106]. The present study showed that TQ inhibited NLRP3 complex components in BC, which came in accordance with the aforementioned studies [101–106].

Along with the current study, various research papers showed that TQ is a possible multi-strike inhibitor of the NLRP3 pathway. It inhibited NF κ B [118], which was pivotal in the priming step of NLRP3 activation [115,116]. Ben-Wen Cui et al. showed that TQ significantly suppressed the protein expression of IL-1 β and the purinergic receptor P2X7R [155], which is a well-known activator of NLRP3 [156]. Various studies reported that the ATP-sensitive K $^{+}$ channel is among the activators of NLRP3, where its inhibition by Glyberide [157] successfully suppressed NLRP3 activation [157,158]. However, the present study showed, for the first time, that TQ was a successful inhibitor to the danger signal

CALR, NLRP3 and its downstream components. Nevertheless, Suddek et al. reported that TQ activated the K⁺ ATP channels [159]. These results came in accordance with those of another study reporting the participation of K⁺ ATP channels in the pharmacological effects of TQ [160]. The aforementioned impacts of TQ on the K⁺ ATP channel might explain the abrupt upregulation and the interesting inhibitory pattern of TQ in PBMCs of HR⁺ and TNBC subtypes (Figure 1D,F, Figures 2D and 3A). In addition, it has been remarked that 20 μM of TQ showed a non-significant elevation in CALR expression after 24 h of treatment in PBMCs of HR⁺ BC patients (Figure 1A), highlighting that the TQ-induced K⁺ ATP channel activation [159] might be responsible for such upregulation. It was believed that mitochondrial and cytoplasmic ATP-dependent K⁺ channels were structurally close [161]. Shigaeva et al. reported that CALR participated in mitochondrial ATP-dependent K⁺ Channel transport, but the exact function and mechanism were unclear [161]. Since TQ activated ATP-sensitive K⁺ channel [159], it would be very interesting to examine the effect of TQ on K⁺ ATP channel/CALR and whether this channel was responsible for the non-significant upregulation of CALR after 24 h of treatment.

Recently, it has been shown throughout various studies that high levels of sPD-L1 are associated with a poor prognosis in TNBC patients [87,88]. In March 2021, ELISA findings showed that sPD-L1 released from the TNBC subtype “MDA-MB231” was higher than that of luminal A T47D and MCF-7 BC cell lines [87]. The current study showed that sPD-L1 released from PBMCs of TNBCs BC patients was significantly higher than that of luminal A (**** $p < 0.0001$) (Figure 7A); these results came in accordance with those of Baojuan Han et al. [87]. For the first time, the present study investigated the impact of increasing TQ concentrations for various durations on protein levels of sPD-L1 released from PBMCs of TNBC patients via ELISA. Fortunately, TQ significantly downregulated sPD-L1 protein release in PBMCs of TNBC patients after 24, 48, and 72 h of treatment (Figure 8B). Although this is the first study that showed the inhibitory impact of TQ on sPD-L1 in PBMCs of TNBC patients, a recent study reported that TQ significantly reduced PD-L1 expression in MDA-MB231 cells [162], which came in accordance with the current results. Thus, collectively, these results suggest that TQ might be a novel adjuvant with atezolizumab (Tecentriq), a PD-L1 inhibitor, in TNBC.

The literature showed that CALR increased PD-L1 levels [125]. In addition, doxorubicin enhanced the CALR and PD-L1 expression in BC cells [126]. In 2019 and 2020, FDA approved the use of atezolizumab (Tecentriq) [163] and pembrolizumab (Keytruda), a PD-1 inhibitor [164], in combination with chemotherapy in the treatment of metastatic PD-L1-positive TNBC patients [165]. Studies showed that IL-1β induced sPD-L1 release in patients with BC [86] and was correlated with significantly short progression-free survival [89]. In addition, NLRP3 contributed to immunosuppression [166] and promoted the expression of PD-L1 in various cancers including BC [59]. Moreover, tumor PD-L1, PD-1, or PD-L1 immunotherapy blockade activated NLRP3 leading to resistance in BC as reviewed by our research group [167], highlighting the fact that CALR/NLRP3 and PD-L1/sPD-L1 might provoke an immunosuppressive/resistance loop in BC. The current findings manifested TQ as a multi-strike inhibitor of CALR, the NLRP3 pathway and sPD-L1 secretion in BC.

The phosphoinositide 3-kinase (PI3K)/AKT pathway is a regulator of pivotal cell functions such as cell proliferation and survival [168]. In BC, PI3K/AKT deregulation via mutations in the PIK3CA gene or inactivation of the tumor suppressor phosphatase and tensin homolog deleted on chromosome 10 (PTEN) have been common in ER⁺ and TNBC patients, respectively [169,170]. It has been reported that an increased PD-L1 expression was mediated via PI3K/AKT activation or a knockdown of PTEN [171]. In addition, PD-L1 activated PI3K/AKT in colorectal cancer [172]. Distinct studies reported that PI3K/AKT increased the levels of matrix metalloproteases (MMP) [173,174]. Surprisingly, tumor cells solubilize the membrane-bound PD-L1 and secrete sPD-L1 [83] by cleavage from the cell surface by MMP [84]. A recent study reported that IL-1β induced sPD-L1 release and increased PD-L1 levels via MMP [86]. Another study came in accordance and showed that IL-1β enhanced MMP production [175,176], leading to PD-L1 solubilization and secretion [84]. In

addition, NLRP3 directly activated MMP [177]. Recent findings reported that PI3K/AKT inhibition suppressed the activation of NLRP3 and decreased its expression [178]. In various cancer studies, TQ has been reported to be a PI3K/AKT inhibitor [179–181], including BC via PTEN upregulation [93,134]. Furthermore, TQ significantly inhibited MMP in numerous cancers such as BC [182], hepatocellular carcinoma [183], prostate cancer [184], renal cell carcinoma [185], neuroblastoma [186], lung cancer [187], and glioblastoma [188]. Recently, FDA approved the use of the oral PI3K inhibitor alpelisib (Piqray) in the treatment of HR+ metastatic BC patients with mutated PIK3CA [189], collectively providing a hint at the potential use of TQ in combination with alpelisib. Also, various in vitro studies should urgently proceed to examine the synergistic impact of combining TQ with alpelisib in distinct TNBC and HR+ BC patients. In addition, it would be worth examining the effect of PI3K/AKT on MMP/sPD-L1 in both HR+ and TNBC with or without TQ. Finally, it is interesting to investigate whether alpelisib would affect the levels of sPD-L1 in TNBC.

The chemokine receptor 2 (CXCR2) has been shown to promote therapy resistance and suppress immunotherapy [190]. The literature reported that CXCR2 activates NLRP3 [191]. Recently, a study performed by our research group showed that doxorubicin increased CXCR2 expression in MDA-MB-231 [190]. In addition, CXCR2 inhibition significantly improved the efficacy of atezolizumab in TNBC in vitro [190]. Another study showed that CXCR2 knockdown decreased PD-L1 levels [192]. Interestingly, 100 μ M of TQ significantly suppressed CXCR2 mRNA levels [193]. Thus, the inhibitory effect of TQ on CXCR2/NLRP3/PD-L1 and sPD-L1 should be further investigated in BC. In addition, the impact of TQ on CALR/NLRP3/IL-1 β /MMP and sPD-L1 needs closer consideration. Also, it would be worth investigating the impact of combining TQ/doxorubicin and atezolizumab in BC.

Cyclin D is frequently deregulated in human cancer and promotes cell division by activating cyclin-dependent kinase 4/6 (CDK 4/6), causing enhanced cell proliferation and BC progression [194,195]. In clinical trials, novel CDK 4/6 inhibitors showed remarkable impacts and received FDA approval for treating BC, such as Ribociclib[®], Palbociclib[®], and Abemaciclib[®] [194]. Studies showed that NLRP3 inhibition suppressed cyclin D1 [196]. In addition, TQ has been reported to induce cell cycle arrest through the inhibition of cyclin E, cyclin D, and cyclin-dependent kinase 2 (CDK-2) in various cancers, as reviewed by our research group [91]. Since the current study showed that TQ significantly inhibited NLRP3 in BC, it would be beneficial to investigate the impact of TQ/cyclin D on CDK4/6 in combination with Abemaciclib[®] in BC, as it might provide a synergistic effect.

To date, no clinical trials have investigated the effect of TQ on cancer in general or BC patients in particular. However, according to clinicaltrials.gov, TQ has been evaluated for its clinical, immunohistochemical, and chemo-preventive impacts on potentially malignant oral lesions. However, the results are not published yet. Patients were divided into three equal groups: Group A was administered buccal tablets containing 10 mg TQ; Group B received buccal 5 mg TQ tablets; Group C was the placebo control group (ClinicalTrials.gov Identifier: NCT03208790).

Among the limitations of the present study is the fact that it only focused on targeting the pro-tumorigenic BC markers comprising CALR, NLRP3 complex components, IL-1 β , and sPD-L1. However, the exact mechanism of how TQ significantly exerted its inhibitory action is still unclear. In addition, it is still questionable whether there is a correlation between PI3K/AKT, CALR/NLRP3/IL-1 β , and MMP/sPD-L1/PD-L1 and cyclin D/CDK4,6 in PBMCs of BC patients. Since TQ significantly inhibited CALR and sPD-L1, it would be beneficial to examine its impact on soluble CALR, PD-L1 expression and protein expressions of CALR, NLRP3, PYCARD, and caspase-1. Moreover, it would be worth examining the inhibitory effect of TQ on NLRP3 expression in PBMCs of HR+ BC patients after 72 h of treatment and IL-1 β in TAMS of TNBC patients. Further in vitro investigation should be preceded to choose TQ's most potent concentration for the most suitable duration in BC. Also, its inhibitory impact should be explored in the HER2+ subtype. The current findings showed that TQ exerted its significant inhibition in PBMCs

and TAMs of BC patients. Thus, investigation should be proceeded in BC tissues and in BC patients.

4. Materials and Methods

4.1. Sample Collection

A total number of 45 BC patients provided written informed consent. Patients diagnosed with TNBC and HR+ luminal A BC were included in the present study. The other BC subtypes were excluded. Patients were stratified into HR+ BC and TNBC patients. All patients were females between the ages of 30 and 79 years. Clinical features are presented in Table 1. Approximately 10 mL of fresh blood was collected from each patient in EDTA tubes to prevent blood coagulation. The current study was approved by the Ethical Committee of the German University in Cairo (approval no. PTX-2019-01-HET) and the Ain Shams University (Cairo, Egypt) and followed the ethical guidelines of the 1975 Declaration of Helsinki.

Table 1. Clinical features of patients with breast cancer.

Patient	Age	Molecular Subtype	Size of Mass, cm	Type	Ki67	Axillary Lymph Node	Treatment
Patient 1	78	Luminal A	3.5 × 3.5 cm	ILC	12%	Negative	Neoadjuvant hormonal therapy Aromatase inhibitor for three months
Patient 2	69	Luminal A	2.5 × 1.8 cm	IDC	3%	Positive	N/A
Patient 3	65	Luminal A	2.5 × 1.6 cm	IDC	15%	Negative	N/A
Patient 4	75	Luminal A	1.5 cm	IDC	7%	Negative	N/A
Patient 5	45	Luminal A	0.8 × 0.4 cm 0.7 × 0.5 cm	IDC	8%	Negative	N/A
Patient 6	53	Luminal A	1.2 × 1 cm	IDC	8%	Positive	N/A
Patient 7	77	Luminal A	1 cm	IDC	5%	Negative	N/A
Patient 8	72	Luminal A	1.2 cm	ILC	12%	Positive	N/A
Patient 9	55	Luminal A	1 × 1.5 cm	IDC	3%	Positive	N/A
Patient 10	30	Luminal A	1.5 cm	IDC	12%	Positive	N/A
Patient 11	60	Luminal A	1 cm	IDC	18%	Positive	Chemotherapy one month before surgery
Patient 12	55	Luminal A	2.8 × 1.6 cm	IDC	12%	Positive	N/A
Patient 13	60	Luminal A	1 cm	IDC	15%	Positive	N/A
Patient 14	60	Luminal A	1.2 cm	IDC	10%	Positive	N/A
Patient 15	65	Luminal A	1 cm	IDC	10%	Positive	N/A
Patient 16	34	Luminal A	1.1 × 1 cm	IDC	12%	Positive	N/A
Patient 17	60	Luminal A	1.5 cm	IDC	7%	Negative	N/A
Patient 18	62	Luminal A	1.3 × 1.5 cm	ILC	15%	Positive	N/A
Patient 19	44	Luminal A	1.2 cm	IDC	14%	Positive	N/A
Patient 20	60	Luminal A	1 cm	IDC	10%	Positive	N/A
Patient 21	64	Luminal A	1.5 cm	ILC	12%	Positive	N/A
Patient 22	44	Luminal A	2.5 × 1.2 cm	IDC	14%	Positive	N/A
Patient 23	62	Luminal A	1.3 cm	IDC	10%	Positive	N/A
Patient 24	47	Luminal A	2 cm	IDC	14%	Positive	N/A
Patient 25	53	Luminal A	1.3 × 1 cm	IDC	12%	Negative	N/A
Patient 26	38	Luminal A	1.5 cm	IDC	7%	Negative	N/A
Patient 27	79	Luminal A	1.5 × 1.2 cm	IDC	8%	Positive	N/A
Patient 28	57	Luminal A	1 cm	IDC	10%	Positive	N/A

Table 1. Cont.

Patient	Age	Molecular Subtype	Size of Mass, cm	Type	Ki67	Axillary Lymph Node	Treatment
Patient 29	59	Luminal A	1.3 cm	IDC	12%	Positive	N/A
Patient 30	66	Luminal A	2 × 1.2 cm	IDC	12%	Positive	N/A
Patient 31	46	TNBCC	2 × 1.5 cm 1.1 × 1 cm	IDC	25%	Positive	N/A
Patient 32	51	TNBCC	2.5 cm	IDC	60%	Negative	N/A
Patient 33	36	TNBCC	1 cm	IDC	50%	Negative	Finished six cycles of chemotherapy
Patient 34	68	TNBCC	2.5 × 3.4 cm	IDC	40%	Negative	N/A
Patient 35	73	TNBCC	3.5 cm	IDC	60%	Negative	Finished neoadjuvant chemotherapy
Patient 36	60	TNBCC	2.5 × 1.5 cm	IDC	50%	Negative	N/A
Patient 37	36	TNBCC	4 × 2 × 2 cm	IDC	70%	Negative	N/A
Patient 38	46	TNBCC	3.5 cm	IDC	50%	Negative	N/A
Patient 39	60	TNBCC	2 × 1.5 cm	IDC	40%	Negative	N/A
Patient 40	72	TNBCC	1.2 cm	IDC	50%	Negative	N/A
Patient 41	39	TNBCC	1.5 cm	IDC	70%	Positive	N/A
Patient 42	54	TNBCC	1 cm	IDC	50%	Negative	N/A
Patient 43	38	TNBCC	2 × 1.5 cm	IDC	40%	Negative	N/A
Patient 44	58	TNBCC	1.5 cm	IDC	70%	Negative	N/A
Patient 45	72	TNBCC	1.2 × 1 cm	IDC	60%	Negative	N/A

Clinical features include the following: age, molecular subtype, tumor size, type, ki67, axillary lymph node status, and treatment. ILC: invasive lobular carcinoma; IDC: invasive ductal carcinoma; N/A: none applicable.

4.2. Peripheral Blood Mononuclear Cell Isolation

Within 2–4 h, PBMCs were isolated from fresh blood by the Ficoll density gradient technique using Histopaque (Sigma-Aldrich gradient, St. Louis, MO, USA). Cell viability of PBMCs was investigated using a Trypan Blue dye exclusion test. The PBMCs of each sample were cryopreserved and stored in a freezer at $-80\text{ }^{\circ}\text{C}$ for later use (Figure 9).

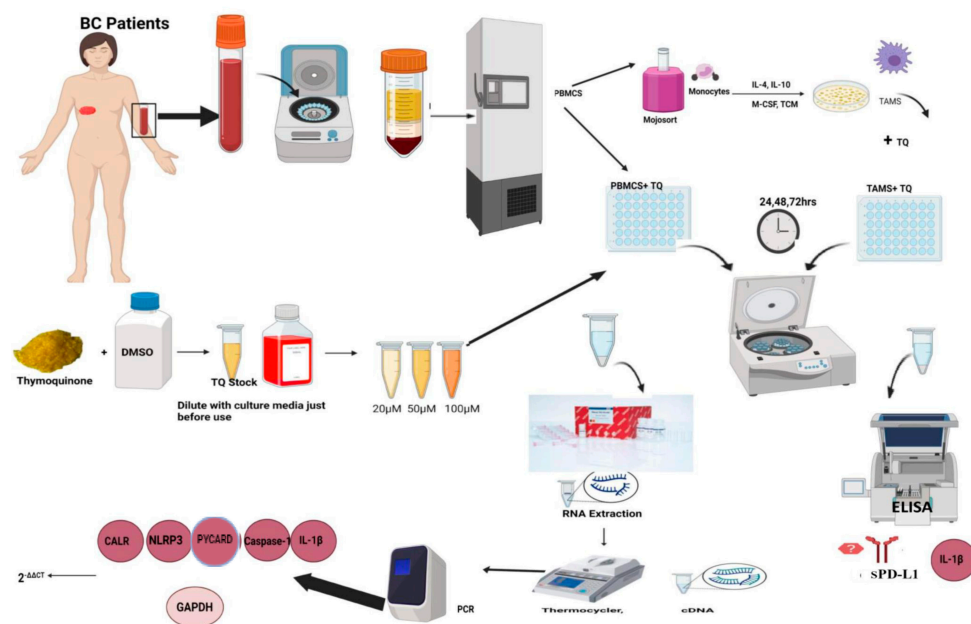


Figure 9. Simplified diagram of methodology. Blood samples were collected from 45 patients with breast cancer (BC): 30 were luminal A and 15 were triple-negative breast cancer patients (TNBC).

Peripheral blood mononuclear cells (PBMCs) were isolated from blood and stored at $-80\text{ }^{\circ}\text{C}$ for future use. Monocytes were extracted from PBMCs using a MojoSort monocyte isolation kit and then differentiated into tumor-associated macrophages (TAMs). Thymoquinone (TQ) stock solution was prepared in dimethyl sulfoxide (DMSO) and was diluted with fresh culture media just before use. According to the literature, 20, 50, and 100 μM concentrations were prepared. PBMCs and TAMs were cultured with the aforementioned TQ concentrations for 24, 48, and 72 h. RNA isolation was conducted with RNeasy Mini Kit (QIAGEN) and then converted into cDNA in the thermocycler. Finally, RT-PCR was used to quantify calreticulin, NLRP3, PYCARD, caspase-1, and IL-1 β . Relative Quantitation (RQ) values were calculated and plotted on the Y-axis against TQ concentrations. The cell culture supernatants were used to measure the secreted protein levels of IL-1 β and sPD-L1 via ELISA. The expression and protein levels were compared to the DMSO control. All experiments were performed in triplicate and data were expressed as the mean \pm standard deviation. Statistical analysis was performed using the GraphPad Prism software version 9.1.1. The data were analyzed using one-way ANOVA, Dunnett's multiple comparisons, and unpaired *t*-test.

4.3. PBMCs Pooling

According to immunohistochemical reports, the current study categorized BC patients into luminal A and TNBC groups. PBMCs of each group of patients were thawed at room temperature, then quickly washed, and centrifuged at 1500 RPM/10 min in cell culture media (RPMI with 10% FBS (Biowest, Nuaille, France) and 1% Pen-Strep (Gibco by Life Technologies, Grand Island, NY, USA)). The supernatant was decanted and pellets were collected (Figure 9).

4.4. MDA-MB231 Culture and Tumor-Conditioned Media (TCM) Preparation

MDA-MB 231 (purchased from Vacsera Egypt) was incubated in Dulbecco's modified Eagle's medium (DMEM) purchased from Lonza, Cologne, Germany (cat. no. 12-604F), supplemented with 4.5 g/L glucose, 4 mmol/L L-glutamine, 10% FBS, and 1% Pen-Strep at $37\text{ }^{\circ}\text{C}$ with an atmosphere of 5% CO_2 and 95% humidity. The cultured cells were allowed to become 80% confluent; then, TCM was harvested and centrifuged to remove suspended cells. After that, the supernatant was collected and stored in a freezer for further use.

4.5. Monocyte Isolation from Hormonal BC Patients and Tumor-Associated Macrophage Differentiation In Vitro

Monocytes were isolated from PBMCs using the MojoSort™ Human CD14+ Monocyte Isolation Kit (Biolegend, San Diego, CA, USA, cat. no. 480019, 480048) following the manufacturer's instructions. The freshly isolated monocytes were plated in a 48-well plate (10,000 cells per well). Monocytes were cultured in TCM and cell culture media with a ratio of 1:1. Additionally, 1 $\mu\text{g}/\text{mL}$ of human interleukin-10 (IL-10) (Shenandoah Biotechnology, Warminster, PA, USA, cat. no. 100-83), 1 $\mu\text{g}/\text{mL}$ of human interleukin-4 (IL-4) (Shenandoah Biotechnology, Warminster, PA, USA, cat. no. 100-09), and 1 $\mu\text{g}/\text{mL}$ of human macrophage colony-stimulating factor (M-CSF) (Shenandoah Biotechnology, Warminster, PA, USA, cat. no. 100-03) were added to the culture media. Monocytes were incubated for seven days. Every other day, medium cytokines were refreshed and cells were microscopically examined; at day 7, TAMs were harvested (3×10^4 cells per well in a 48-well plate) (Figure 9).

4.6. Flow Cytometry

At day 7, flow cytometry was performed using anti-CD163 FITC in accordance with the manufacturer's instructions (cat. no. sc.33715, Santa Cruz Biotechnology, Dallas, TX, USA) to ensure successful TAMs differentiation. Briefly, cells were dissociated, followed by single-cell suspension preparation (240,000 cells/tube). Cells were washed with 2 mL (PBS 1% FBS) and centrifuged for 5 min; then, the supernatant was discarded. After that, 1.2 μg anti-CD163 FITC was added (5 $\mu\text{g}/1$ million cells) and incubated for 30 min at 4° degrees. Finally, analysis was performed using CytoFLEX flow cytometry.

4.7. Thymoquinone (TQ) Preparations

First, 20, 50, and 100 mM stock solutions of TQ (Acros Organics, Geel, Belgium code:305070010, GC: 98.6%) were dissolved in dimethyl sulfoxide (DMSO) (Loba Chemie, Mumbai, India) and stored at -80°C . The TQ stock solutions were diluted in fresh cell culture media into (20, 50, and 100 μM) just before use. Note that the percentage of DMSO was 0.1% in order to not be toxic to cells.

4.8. PBMCs and TAMs Coculture with TQ

In a pyrogen-free 48-well plate, PBMCs were cocultured with TQ (3×10^6 cells per mL) at increasing concentrations (20, 50, and 100 μM) and durations (24, 48, and 72 h), as shown in Figure 9. TAMs were cocultured (3×10^4 cells per well) with the aforementioned concentrations for 24 h. Notably, each TQ concentration was cultured in triplicate.

4.9. RNA Extraction, Complementary DNA (cDNA), and Quantified Real-Time Polymerase Chain Reaction (qRT-PCR)

RNA isolation was performed using the RNeasy Mini Kit (QIAGEN, Hilden, Germany, cat. no. 74104). Total RNA was then converted to cDNA by the Thermo Scientific RevertAid First Strand cDNA Synthesis Kit. The relative expressions of CALR (Hs00189032_m1, cat. no. 4331182), NLRP3 (Hs00918082_m1, cat. no.4331182), PYCARD (Hs01547324_gh, cat. no. 4331182), caspase-1 (Hs00354836_m1, cat no. 4331182), IL-1 β (Hs01555410_m1, cat. no. 4331182), and GAPDH (Hs99999905_m1 VIC, cat no. 4326317E) (as a housekeeping gene for normalization) were amplified and quantified on a StepOne Real-Time PCR instrument (Applied Biosystems; Thermo Fisher Scientific Inc., Waltham, MA USA) using TaqMan Real-time PCR (Applied Biosystems; Thermo Fisher Scientific Inc., Waltham, MA USA). For each sample, a reaction mix was prepared according to the manufacturer's instructions, and 4 μL of the respective cDNA was added. The RT-qPCR run was performed in the standard mode, which consists of two stages: the first stage, where the Taq polymerase enzyme was activated for 10 min at 95°C , and the second stage, which consisted of 40 amplification cycles. Notably, all PCR reactions, including controls, were run in triplicate reactions. Values were calculated as RQ represented as $2^{-\Delta\Delta\text{CT}}$ (Figure 9).

4.10. Enzyme-Linked Immunosorbent Assay

The protein release of IL-1 β and sPD-L1 in cell culture supernatants was conducted following manufacturer's instructions using the human IL-1 β ELISA kit (cat. no. E-EL-H0149, E-lab science, Houston, TX, USA) and the PD-L1 human ELISA kit (cat. no. K1025-100, Biovision, Milpitas, CA, USA).

4.11. Statistical Analysis

All experiments were performed in triplicate and data are expressed as the mean \pm standard deviation. Statistical analysis was performed using the GraphPad Prism software version 9.1.1. The data were analyzed using one-way ANOVA and Dunnett's multiple comparisons to compare each treated column and the DMSO control column. The column chart was plotted, RQ values were on the Y-axis, and TQ concentrations were drawn on the X-axis. To compare the DMSO control and the two BC subtypes (TNBC and luminal A HR+ BC), the unpaired *t*-test was used (**** $p < 0.0001$; *** $p < 0.001$; ** $p < 0.01$; * $p < 0.05$).

5. Conclusions and Future Insights

The present findings showed that TQ is a novel significant inhibitor of CALR, NLRP3 complex components, as well as IL-1 β and sPD-L1 in TAMs and PBMCs of HR+ and TNBC, respectively. The current study sheds light on targeting multiple pro-tumorigenic BC markers using TQ. In addition, it urgently recommends exploring TQ's clinical impact on HR+ and TNBC patients alone and in combination with atezolizumab. Collectively, TQ might be an excellent multi-strike adjuvant and a potential immunotherapeutic in both HR+ and TNBC patients for future investigation.

Author Contributions: S.E. performed the experiments, participated in its design, wrote the manuscript, and analyzed the results. R.A.E. co-supervised the project, facilitated the blood collection procedures, and provided clinical data for the patients. H.M.E.T. is the main supervisor of this research work; she designed the experiments, revised the manuscript, and performed the statistical analysis. Finally, all authors contributed to writing the manuscript. All authors have read and agreed to the published version of the manuscript.

Funding: This research received no external funding.

Institutional Review Board Statement: The current study was approved by the Ethical Committee of the German University in Cairo (approval no. PTX-2019-01-HET) and Ain Shams University (Cairo, Egypt) and followed the ethical guidelines of the 1975 Declaration of Helsinki.

Informed Consent Statement: The studies involving human participants were reviewed and approved by the German University in Cairo and the Ain Shams University Ethical Committees. The study followed the ethical guidelines of the 1975 Declaration of Helsinki. The patients/participants provided written informed consent to participate in this study. The work described in this article is original, neither submitted to nor published in other journals.

Data Availability Statement: The data presented in this study are available upon request from the corresponding author.

Acknowledgments: Not applicable.

Conflicts of Interest: The authors declare no conflict of interest.

References

1. Sung, H.; Ferlay, J.; Siegel, R.L.; Laversanne, M.; Soerjomataram, I.; Jemal, A.; Bray, F. Global Cancer Statistics 2020: GLOBOCAN Estimates of Incidence and Mortality Worldwide for 36 Cancers in 185 Countries. *CA. Cancer J. Clin.* **2021**, *71*, 209–249. [[CrossRef](#)]
2. Cho, N. Molecular subtypes and imaging phenotypes of breast cancer. *Ultrasonography* **2016**, *35*, 281–288. [[CrossRef](#)]
3. Cichon, M.A.; Degnim, A.C.; Visscher, D.W.; Radisky, D.C. Microenvironmental influences that drive progression from benign breast disease to invasive breast cancer. *J. Mammary Gland Biol. Neoplasia* **2010**, *15*, 389–397. [[CrossRef](#)]
4. Dumeaux, V.; Fjukstad, B.; Fjosne, H.E.; Frantzen, J.O.; Holmen, M.M.; Rodegerdts, E.; Schlichting, E.; Børresen-Dale, A.L.; Bongo, L.A.; Lund, E.; et al. Interactions between the tumor and the blood systemic response of breast cancer patients. *PLoS Comput. Biol.* **2017**, *13*, e1005680. [[CrossRef](#)]
5. Danforth, D.N. The role of chronic inflammation in the development of breast cancer. *Cancers* **2021**, *13*, 3918. [[CrossRef](#)]
6. Batalha, S.; Ferreira, S.; Brito, C. The peripheral immune landscape of breast cancer: Clinical findings and in vitro models for biomarker discovery. *Cancers* **2021**, *13*, 1305. [[CrossRef](#)]
7. Moradpoor, R.; Gharebaghian, A.; Shahi, F.; Mousavi, A.; Salari, S.; Akbari, M.E.; Ajdari, S.; Salimi, M. Identification and Validation of Stage-Associated PBMC Biomarkers in Breast Cancer Using MS-Based Proteomics. *Front. Oncol.* **2020**, *10*, 1101. [[CrossRef](#)]
8. Dumeaux, V.; Ursini-Siegel, J.; Flatberg, A.; Fjosne, H.E.; Frantzen, J.O.; Holmen, M.M.; Rodegerdts, E.; Schlichting, E.; Lund, E. Peripheral blood cells inform on the presence of breast cancer: A population-based case-control study. *Int. J. Cancer* **2015**, *136*, 656–667. [[CrossRef](#)]
9. Aguilar-Cazares, D.; Chavez-Dominguez, R.; Marroquin-Muciño, M.; Perez-Medina, M.; Benito-Lopez, J.J.; Camarena, A.; Rumbo-Nava, U.; Lopez-Gonzalez, J.S. The systemic-level repercussions of cancer-associated inflammation mediators produced in the tumor microenvironment. *Front. Endocrinol.* **2022**, *13*, 929572. [[CrossRef](#)]
10. Hernandez, C.; Huebener, P.; Schwabe, R.F. Damage-associated molecular patterns in cancer: A double-edged sword. *Oncogene* **2016**, *35*, 5931–5941. [[CrossRef](#)]
11. Kim, R.; Kin, T. Current and future therapies for immunogenic cell death and related molecules to potentially cure primary breast cancer. *Cancers* **2021**, *13*, 4756. [[CrossRef](#)]
12. Kwa, M.J.; Adams, S. Checkpoint inhibitors in triple-negative breast cancer (TNBC): Where to go from here. *Cancer* **2018**, *124*, 2086–2103. [[CrossRef](#)]
13. Peng, Z.; Su, P.; Yang, Y.; Yao, X.; Zhang, Y.; Jin, F.; Yang, B. Identification of CTLA-4 associated with tumor microenvironment and competing interactions in triple negative breast cancer by co-expression network analysis. *J. Cancer* **2020**, *11*, 6365–6375. [[CrossRef](#)]
14. Hammerl, D.; Smid, M.; Timmermans, A.M.; Sleijfer, S.; Martens, J.W.M.; Debets, R. Breast cancer genomics and immunological markers to guide immune therapies. *Semin. Cancer Biol.* **2018**, *52*, 178–188. [[CrossRef](#)]
15. Grivnenkov, S.I.; Greten, F.R.; Karin, M. Immunity, Inflammation, and Cancer. *Cell* **2010**, *140*, 883–899. [[CrossRef](#)]
16. Roh, J.S.; Sohn, D.H. Damage-associated molecular patterns in inflammatory diseases. *Immune Netw.* **2018**, *18*, e27. [[CrossRef](#)]
17. Fucikova, J.; Spisek, R.; Kroemer, G.; Galluzzi, L. Calreticulin and cancer. *Cell Res.* **2021**, *31*, 5–16. [[CrossRef](#)]

18. Ocadlikova, D.; Lecciso, M.; Isidori, A.; Loscocco, F.; Visani, G.; Amadori, S.; Cavo, M.; Curti, A. Chemotherapy-Induced Tumor Cell Death at the Crossroads Between Immunogenicity and Immunotolerance: Focus on Acute Myeloid Leukemia. *Front. Oncol.* **2019**, *9*, 1004. [[CrossRef](#)]
19. Gameiro, S.R.; Jammeh, M.L.; Wattenberg, M.M.; Tsang, K.Y.; Ferrone, S.; Hodge, J.W. Radiation-induced immunogenic modulation of tumor enhances antigen processing and calreticulin exposure, resulting in enhanced T-cell killign. *Oncotarget* **2014**, *5*, 403–416. [[CrossRef](#)]
20. Zhou, H.; Forveille, S.; Sauvat, A.; Yamazaki, T.; Senovilla, L.; Ma, Y.; Liu, P.; Yang, H.; Bezu, L.; Müller, K.; et al. The oncolytic peptide LTX-315 triggers immunogenic cell death. *Cell Death Dis.* **2016**, *7*, e2134. [[CrossRef](#)]
21. Gardai, S.J.; McPhillips, K.A.; Frasch, S.C.; Janssen, W.J.; Starefeldt, A.; Murphy-Ullrich, J.E.; Bratton, D.L.; Oldenborg, P.A.; Michalak, M.; Henson, P.M. Cell-surface calreticulin initiates clearance of viable or apoptotic cells through trans-activation of LRP on the phagocyte. *Cell* **2005**, *123*, 321–334. [[CrossRef](#)]
22. Arosa, F.A.; De Jesus, O.; Porto, G.; Carmo, A.M.; De Sousa, M. Calreticulin is expressed on the cell surface of activated human peripheral blood T lymphocytes in association with major histocompatibility complex class I molecules. *J. Biol. Chem.* **1999**, *274*, 16917–16922. [[CrossRef](#)]
23. Feng, M.; Chen, J.Y.; Weissman-Tsakamoto, R.; Volkmer, J.P.; Ho, P.Y.; McKenna, K.M.; Cheshier, S.; Zhang, M.; Guo, N.; Gip, P.; et al. Macrophages eat cancer cells using their own calreticulin as a guide: Roles of TLR and Btk. *Proc. Natl. Acad. Sci. USA* **2015**, *112*, 2145–2150. [[CrossRef](#)]
24. Zeng, G.; Aldridge, M.E.; Tian, X.; Seiler, D.; Zhang, X.; Jin, Y.; Rao, J.; Li, W.; Chen, D.; Langford, M.P.; et al. Dendritic Cell Surface Calreticulin Is a Receptor for NY-ESO-1: Direct Interactions between Tumor-Associated Antigen and the Innate Immune System. *J. Immunol.* **2006**, *177*, 3582–3589. [[CrossRef](#)]
25. Zhou, P.; Teruya-Feldstein, J.; Lu, P.; Fleisher, M.; Olshen, A.; Comenzo, R.L. Calreticulin expression in the clonal plasma cells of patients with systemic light-chain (AL-) amyloidosis is associated with response to high-dose melphalan. *Blood* **2008**, *111*, 549–557. [[CrossRef](#)]
26. Zheng, Y.; Li, C.; Xin, P.; Peng, Q.; Zhang, W.; Liu, S.; Zhu, X. Calreticulin increases growth and progression of natural killer/T-cell lymphoma. *Aging* **2020**, *12*, 23822–23835. [[CrossRef](#)]
27. Osman, R.; Tacnet-Delorme, P.; Kleman, J.P.; Millet, A.; Frchet, P. Calreticulin release at an early stage of death modulates the clearance by macrophages of apoptotic cells. *Front. Immunol.* **2017**, *8*, 1034. [[CrossRef](#)]
28. Aydın, E.B.; Aydın, M.; Sezginürk, M.K. A Simple and Low-Cost Electrochemical Immunosensor for Ultrasensitive Determination of Calreticulin Biomarker in Human Serum. *Macromol. Biosci.* **2023**, *23*, e2200390. [[CrossRef](#)]
29. SUN, M.; YANG, G.; ZHAO, Y.; QU, F. Screening of Aptamer for Breast Cancer Biomarker Calreticulin and Its Application to Detection of Serum and Recognition of Breast Cancer Cell. *Chin. J. Anal. Chem.* **2020**, *48*, 642–649. [[CrossRef](#)]
30. Cruz-Ramos, E.; Sandoval-Hernández, A.; Tecalco-Cruz, A.C. Differential expression and molecular interactions of chromosome region maintenance 1 and calreticulin exportins in breast cancer cells. *J. Steroid Biochem. Mol. Biol.* **2019**, *185*, 7–16. [[CrossRef](#)]
31. Erić, A.; Jurić, Z.; Milovanović, Z.; Marković, I.; Inić, M.; Stanojević-Bakić, N.; Vojinović-Golubović, V. Effects of humoral immunity and calreticulin overexpression on postoperative course in breast cancer. *Pathol. Oncol. Res.* **2009**, *15*, 89–90. [[CrossRef](#)]
32. Gromov, P.; Gromova, I.; Bunkenborg, J.; Cabezon, T.; Moreira, J.M.A.; Timmermans-Wielenga, V.; Roepstorff, P.; Rank, F.; Celis, J.E. Up-regulated Proteins in the Fluid Bathing the Tumour Cell Microenvironment as Potential Serological Markers for Early Detection of Cancer of the Breast. *Mol. Oncol.* **2010**, *4*, 65–89. [[CrossRef](#)]
33. Lwin, Z.M.; Guo, C.; Salim, A.; Yip, G.W.C.; Chew, F.T.; Nan, J.; Thike, A.A.; Tan, P.H.; Bay, B.H. Clinicopathological significance of calreticulin in breast invasive ductal carcinoma. *Mod. Pathol.* **2010**, *23*, 1559–1566. [[CrossRef](#)]
34. Zamanian, M.; Qader Hamadneh, L.A.; Veerakumarasivam, A.; Abdul Rahman, S.; Shohaimi, S.; Rosli, R. Calreticulin mediates an invasive breast cancer phenotype through the transcriptional dysregulation of p53 and MAPK pathways. *Cancer Cell Int.* **2016**, *16*, 56. [[CrossRef](#)]
35. Yang, Y.; Wang, H.; Kouadir, M.; Song, H.; Shi, F. Recent advances in the mechanisms of NLRP3 inflammasome activation and its inhibitors. *Cell Death Dis.* **2019**, *10*, 128. [[CrossRef](#)]
36. Liu, Y.; Wei, W.; Wang, Y.; Wan, C.; Bai, Y.; Sun, X.; Ma, J.; Zheng, F. TNF- α /calreticulin dual signaling induced NLRP3 inflammasome activation associated with HuR nucleocytoplasmic shuttling in rheumatoid arthritis. *Inflamm. Res.* **2019**, *68*, 597–611. [[CrossRef](#)]
37. Jiang, Z.; Chen, Z.; Hu, L.; Qiu, L.; Zhu, L. Calreticulin Blockade Attenuates Murine Acute Lung Injury by Inducing Polarization of M2 Subtype Macrophages. *Front. Immunol.* **2020**, *11*, 11. [[CrossRef](#)]
38. Zhang, B.; Xu, D.; She, L.; Wang, Z.; Yang, N.; Sun, R.; Zhang, Y.; Yan, C.; Wei, Q.; Aa, J.; et al. Silybin inhibits NLRP3 inflammasome assembly through the NAD⁺/SIRT2 pathway in mice with nonalcoholic fatty liver disease. *FASEB J.* **2018**, *32*, 757–767. [[CrossRef](#)]
39. Mónaco, A.; Chilibroste, S.; Yim, L.; Chabalgoity, J.A.; Moreno, M. Inflammasome activation, NLRP3 engagement and macrophage recruitment to tumor microenvironment are all required for Salmonella antitumor effect. *Cancer Immunol. Immunother.* **2022**, *71*, 2141–2150. [[CrossRef](#)]
40. Chen, H.; Zhang, X.; Liao, N.; Mi, L.; Peng, Y.; Liu, B.; Zhang, S.; Wen, F. Enhanced expression of NLRP3 inflammasome-related inflammation in diabetic retinopathy. *Investig. Ophthalmol. Vis. Sci.* **2018**, *59*, 978–985. [[CrossRef](#)]

41. Silva, M.D.S.; Lopes, J.A.; Paloschi, M.V.; Boeno, C.N.; Rego, C.M.A.; de Oliveira Sousa, O.; Santana, H.M.; dos Reis, V.P.; Serrath, S.N.; Setúbal, S.d.S.; et al. NLRP3 inflammasome activation in human peripheral blood mononuclear cells induced by venoms secreted PLA2s. *Int. J. Biol. Macromol.* **2022**, *202*, 597–607. [[CrossRef](#)]
42. Zhu, J.; Wu, S.; Hu, S.; Li, H.; Li, M.; Geng, X.; Wang, H. NLRP3 inflammasome expression in peripheral blood monocytes of coronary heart disease patients and its modulation by rosuvastatin. *Mol. Med. Rep.* **2019**, *20*, 1826–1836. [[CrossRef](#)]
43. Kummer, J.A.; Broekhuizen, R.; Everett, H.; Agostini, L.; Kuijk, L.; Martinon, F.; Van Bruggen, R.; Tschopp, J. Inflammasome components NALP 1 and 3 show distinct but separate expression profiles in human tissues suggesting a site-specific role in the inflammatory response. *J. Histochem. Cytochem.* **2007**, *55*, 443–452. [[CrossRef](#)]
44. Sand, J.; Haertel, E.; Biedermann, T.; Contassot, E.; Reichmann, E.; French, L.E.; Werner, S.; Beer, H.D. Expression of inflammasome proteins and inflammasome activation occurs in human, but not in murine keratinocytes article. *Cell Death Dis.* **2018**, *9*, 24. [[CrossRef](#)]
45. Hsieh, C.W.; Chen, Y.M.; Lin, C.C.; Tang, K.T.; Chen, H.H.; Hung, W.T.; Lai, K.L.; Chen, D.Y. Elevated expression of the NLRP3 inflammasome and its correlation with disease activity in adult-onset still disease. *J. Rheumatol.* **2017**, *44*, 1142–1150. [[CrossRef](#)]
46. Peelen, E.; Damoiseaux, J.; Muris, A.H.; Knippenberg, S.; Smolders, J.; Hupperts, R.; Thewissen, M. Increased inflammasome related gene expression profile in PBMC may facilitate T helper 17 cell induction in multiple sclerosis. *Mol. Immunol.* **2015**, *63*, 521–529. [[CrossRef](#)]
47. Qiu, D.; Zhang, D.; Yu, Z.; Jiang, Y.; Zhu, D. Bioinformatics approach reveals the critical role of the NOD-like receptor signaling pathway in COVID-19-associated multiple sclerosis syndrome. *J. Neural Transm.* **2022**, *129*, 1031–1038. [[CrossRef](#)]
48. Shamsabadi, R.M.; Basafa, S.; Yarahmadi, R.; Goorani, S.; Khani, M.; Kamarehei, M.; Hossein Kiani, A. Elevated Expression of NLRP1 and IPAF Are Related to Oral Pemphigus Vulgaris Pathogenesis. *Inflammation* **2015**, *38*, 205–208. [[CrossRef](#)]
49. Ugurel, E.; Erdag, E.; Kucukali, C.I.; Olcay, A.; Sanli, E.; Akbayir, E.; Kurtuncu, M.; Gunduz, T.; Yilmaz, V.; Tuzun, E.; et al. Enhanced NLRP3 and DEFA1B expression during the active stage of parenchymal neuro-behçet's disease. *In Vivo* **2019**, *33*, 1493–1497. [[CrossRef](#)]
50. Scianaro, R.; Insalaco, A.; Bracci Laudiero, L.; De Vito, R.; Pezzullo, M.; Teti, A.; De Benedetti, F.; Prencipe, G. Deregulation of the IL-1 β axis in chronic recurrent multifocal osteomyelitis. *Pediatr. Rheumatol.* **2014**, *12*, 30. [[CrossRef](#)]
51. Akhlaghi, M.; Karrabi, M.; Atabti, H.; Raoofi, A.; Mousavi Khaneghah, A. Investigation of the role of IL18, IL-1 β and NLRP3 inflammasome in reducing expression of FLG-2 protein in Psoriasis vulgaris skin lesions. *Biotech. Histochem.* **2022**, *97*, 277–283. [[CrossRef](#)]
52. Wu, X.; Cakmak, S.; Wortmann, M.; Hakimi, M.; Zhang, J.; Böckler, D.; Dihlmann, S. Sex-and disease-specific inflammasome signatures in circulating blood leukocytes of patients with abdominal aortic aneurysm. *Mol. Med.* **2016**, *22*, 508–518. [[CrossRef](#)]
53. Wu, X.; Hakimi, M.; Wortmann, M.; Zhang, J.; Böckler, D.; Dihlmann, S. Gene expression of inflammasome components in peripheral blood mononuclear cells (PBMC) of vascular patients increases with age. *Immun. Ageing* **2015**, *12*, 15. [[CrossRef](#)] [[PubMed](#)]
54. Ferlazzo, N.; Currò, M.; Isola, G.; Maggio, S.; Bertuccio, M.P.; Trovato-Salinaro, A.; Matarese, G.; Alibrandi, A.; Caccamo, D.; Ientile, R. Changes in the biomarkers of oxidative/nitrosative stress and endothelial dysfunction are associated with cardiovascular risk in periodontitis patients. *Curr. Issues Mol. Biol.* **2021**, *43*, 704–715. [[CrossRef](#)] [[PubMed](#)]
55. Pereira, N.d.S.; Queiroga, T.B.D.; Nunes, D.F.; Andrade, C.d.M.; Nascimento, M.S.L.; Do-Valle-Matta, M.A.; da Câmara, A.C.J.; Galvão, L.M.d.C.; Guedes, P.M.M.; Chiari, E. Innate immune receptors over expression correlate with chronic chagasic cardiomyopathy and digestive damage in patients. *PLoS Negl. Trop. Dis.* **2018**, *12*, e0006589. [[CrossRef](#)]
56. Rodrigues, T.S.; de Sá, K.S.G.; Ishimoto, A.Y.; Becerra, A.; Oliveira, S.; Almeida, L.; Gonçalves, A.V.; Perucello, D.B.; Andrade, W.A.; Castro, R.; et al. Inflammasomes are activated in response to SARS-cov-2 infection and are associated with COVID-19 severity in patients. *J. Exp. Med.* **2020**, *218*, e20201707. [[CrossRef](#)] [[PubMed](#)]
57. Vakrakou, A.G.; Boiu, S.; Ziakas, P.D.; Xingi, E.; Boleti, H.; Manoussakis, M.N. Systemic activation of NLRP3 inflammasome in patients with severe primary Sjögren's syndrome fueled by inflammagenic DNA accumulations. *J. Autoimmun.* **2018**, *91*, 23–33. [[CrossRef](#)]
58. Pakvisal, N.; Kongkaviton, P.; Sathitruangsak, C.; Pornpattanak, N.; Boonsirikamchai, P.; Ouwongprayoon, P.; Aporntewan, C.; Chantranuwatana, P.; Mutirangura, A.; Vinayanuwattikun, C. Differential expression of immune-regulatory proteins C5AR1, CLEC4A and NLRP3 on peripheral blood mononuclear cells in early-stage non-small cell lung cancer patients. *Sci. Rep.* **2022**, *12*, 18439. [[CrossRef](#)]
59. Ding, Y.; Yan, Y.; Dong, Y.; Xu, J.; Su, W.; Shi, W.; Zou, Q.; Yang, X. NLRP3 promotes immune escape by regulating immune checkpoints: A pan-cancer analysis. *Int. Immunopharmacol.* **2022**, *104*, 108512. [[CrossRef](#)] [[PubMed](#)]
60. Felicetti, F.; Aimaretti, E.; Dal Bello, F.; Gatti, F.; Godono, A.; Saba, F.; Einaudi, G.; Collino, M.; Fagioli, F.; Aragno, M.; et al. Advanced glycation end products and their related signaling cascades in adult survivors of childhood Hodgkin lymphoma: A possible role in the onset of late complications. *Free Radic. Biol. Med.* **2022**, *178*, 76–82. [[CrossRef](#)]
61. Saponaro, C.; Scarpi, E.; Sonnessa, M.; Cioffi, A.; Buccino, F.; Giotta, F.; Pastena, M.I.; Zito, F.A.; Mangia, A. Prognostic Value of NLRP3 Inflammasome and TLR4 Expression in Breast Cancer Patients. *Front. Oncol.* **2021**, *11*, 705331. [[CrossRef](#)] [[PubMed](#)]
62. Wang, Y.; Zhang, H.; Xu, Y.; Peng, T.; Meng, X.; Zou, F. NLRP3 induces the autocrine secretion of IL-1 β to promote epithelial-mesenchymal transition and metastasis in breast cancer. *Biochem. Biophys. Res. Commun.* **2021**, *560*, 72–79. [[CrossRef](#)] [[PubMed](#)]

63. Zhang, L.; Li, H.; Zang, Y.; Wang, F. NLRP3 inflammasome inactivation driven by miR-223-3p reduces tumor growth and increases anticancer immunity in breast cancer. *Mol. Med. Rep.* **2019**, *19*, 2180–2188. [[CrossRef](#)] [[PubMed](#)]
64. Hu, Q.; Zhao, F.; Guo, F.; Wang, C.; Fu, Z. Polymeric Nanoparticles Induce NLRP3 Inflammasome Activation and Promote Breast Cancer Metastasis. *Macromol. Biosci.* **2017**, *17*, 1700273. [[CrossRef](#)]
65. Yentis, S.M.; Rowbottom, A.W.; Riches, P.G. Detection of cytoplasmic IL-1 β in peripheral blood mononuclear cells from intensive care unit (ICU) patients. *Clin. Exp. Immunol.* **1995**, *100*, 330–335. [[CrossRef](#)]
66. Perez, R.L.; Roman, J. Fibrin enhances the expression of IL-1 beta by human peripheral blood mononuclear cells. Implications in pulmonary inflammation. *J. Immunol.* **1995**, *154*, 1879–1887. [[CrossRef](#)]
67. Ferentinos, P.; Maratou, E.; Antoniou, A.; Serretti, A.; Smyrnis, N.; Moutsatsou, P. Interleukin-1 Beta in Peripheral Blood Mononuclear Cell Lysates as a Longitudinal Biomarker of Response to Antidepressants: A Pilot Study. *Front. Psychiatry* **2021**, *12*, 801738. [[CrossRef](#)]
68. Adachi, M.; Inoue, H.; Arinaga, S.; Li, J.; Ueo, H.; Mori, M.; Akiyoshi, T. Quantitative analysis of cytokine mRNA expression in peripheral blood mononuclear cells following treatment with interleukin-2. *Cancer Immunol. Immunother.* **1997**, *44*, 329–334. [[CrossRef](#)]
69. Autenshlyus, A.I.; Davletova, K.I.; Mikhaylova, E.S.; Proskura, A.V.; Varaksin, N.A.; Bogachuk, A.P.; Sidorov, S.V.; Lyakhovich, V.V.; Lipkin, V.M. Influence of Internal and External Factors on the Production of Cytokines by Peripheral Blood Cells in Breast Cancer. *Dokl. Biochem. Biophys.* **2020**, *493*, 178–180. [[CrossRef](#)]
70. Cai, S.; Zheng, J.; Song, H.; Wu, H.; Cai, W. Relationship between serum TGF- β 1, MMP-9 and IL-1 β and pathological features and prognosis in breast cancer. *Front. Genet.* **2023**, *13*, 1095338. [[CrossRef](#)]
71. Alipour, S.; Khalighfard, S.; Khori, V.; Amirani, T.; Tajaldini, M.; Dehghan, M.; Sadani, S.; Omranipour, R.; Vahabzadeh, G.; Eslami, B.; et al. Innovative targets of the lncRNA-miR-mRNA network in response to low-dose aspirin in breast cancer patients. *Sci. Rep.* **2022**, *12*, 12054. [[CrossRef](#)]
72. Panis, C.; Victorino, V.J.; Herrera, A.C.S.A.; Freitas, L.F.; De Rossi, T.; Campos, F.C.; Colado Simão, A.N.; Barbosa, D.S.; Pinge-Filho, P.; Cecchini, R.; et al. Differential oxidative status and immune characterization of the early and advanced stages of human breast cancer. *Breast Cancer Res. Treat.* **2012**, *133*, 881–888. [[CrossRef](#)] [[PubMed](#)]
73. Woo, Y.; Kim, H.; Kim, K.C.; Han, J.A.; Jung, Y.J. Tumor-secreted factors induce IL-1 β maturation via the glucose-mediated synergistic axis of mTOR and NF- κ B pathways in mouse macrophages. *PLoS ONE* **2018**, *13*, e0209653. [[CrossRef](#)] [[PubMed](#)]
74. Ren, X.; Ren, P.; Luo, S.; Ji, Q.; Xu, M.; Lu, N.; Wang, Y. Detection and analysis of phenotypes of tumor-associated macrophages in mouse model of spontaneous breast cancer. *Xi Bao Yu Fen Zi Mian Yi Xue Za Zhi* **2017**, *33*, 721–725. [[PubMed](#)]
75. Qin, Q.; Ji, H.; Li, D.; Zhang, H.; Zhang, Z.; Zhang, Q. Tumor-associated macrophages increase COX-2 expression promoting endocrine resistance in breast cancer via the PI3K/Akt/mTOR pathway. *Neoplasma* **2021**, *68*, 938–946. [[CrossRef](#)] [[PubMed](#)]
76. Jiménez-Garduño, A.M.; Mendoza-Rodríguez, M.G.; Urrutia-Cabrera, D.; Domínguez-Robles, M.C.; Pérez-Yépez, E.A.; Ayala-Sumuano, J.T.; Meza, I. IL-1 β induced methylation of the estrogen receptor ER α gene correlates with EMT and chemoresistance in breast cancer cells. *Biochem. Biophys. Res. Commun.* **2017**, *490*, 780–785. [[CrossRef](#)]
77. Rani, A.; Stebbing, J.; Giamas, G.; Murphy, J. Endocrine resistance in hormone receptor positive breast cancer—from mechanism to therapy. *Front. Endocrinol.* **2019**, *10*, 245. [[CrossRef](#)]
78. Wein, L.; Loi, S. Mechanisms of resistance of chemotherapy in early-stage triple negative breast cancer (TNBC). *Breast* **2017**, *34*, S27–S30. [[CrossRef](#)]
79. Schütz, F.; Stefanovic, S.; Mayer, L.; Von Au, A.; Domschke, C.; Sohn, C. PD-1/PD-L1 Pathway in Breast Cancer. *Oncol. Res. Treat.* **2017**, *40*, 294–297. [[CrossRef](#)]
80. Dong, Y.; Sun, Q.; Zhang, X. PD-1 and its ligands are important immune checkpoints in cancer. *Oncotarget* **2017**, *8*, 2171–2186. [[CrossRef](#)]
81. Pardoll, D.M. The blockade of immune checkpoints in cancer immunotherapy. *Nat. Rev. Cancer* **2012**, *12*, 252–264. [[CrossRef](#)] [[PubMed](#)]
82. Katz, H.; Alsharedi, M. Immunotherapy in triple-negative breast cancer. *Med. Oncol.* **2018**, *35*, 13. [[CrossRef](#)] [[PubMed](#)]
83. Frigola, X.; Inman, B.A.; Lohse, C.M.; Krco, C.J.; Cheville, J.C.; Thompson, R.H.; Leibovich, B.; Blute, M.L.; Dong, H.; Kwon, E.D. Identification of a soluble form of B7-H1 that retains immunosuppressive activity and is associated with aggressive renal cell carcinoma. *Clin. Cancer Res.* **2011**, *17*, 1915–1923. [[CrossRef](#)] [[PubMed](#)]
84. Chen, Y.; Wang, Q.; Shi, B.; Xu, P.; Hu, Z.; Bai, L.; Zhang, X. Development of a sandwich ELISA for evaluating soluble PD-L1 (CD274) in human sera of different ages as well as supernatants of PD-L1 + cell lines. *Cytokine* **2011**, *56*, 231–238. [[CrossRef](#)] [[PubMed](#)]
85. Asanuma, K.; Nakamura, T.; Hayashi, A.; Okamoto, T.; Iino, T.; Asanuma, Y.; Hagi, T.; Kita, K.; Nakamura, K.; Sudo, A. Soluble programmed death-ligand 1 rather than PD-L1 on tumor cells effectively predicts metastasis and prognosis in soft tissue sarcomas. *Sci. Rep.* **2020**, *10*, 9077. [[CrossRef](#)]
86. Baggio, C.; Ramaschi, G.E.; Oliviero, F.; Ramonda, R.; Sfriso, P.; Trevisi, L.; Cignarella, A.; Bolego, C. Sex-dependent PD-L1/sPD-L1 trafficking in human endothelial cells in response to inflammatory cytokines and VEGF. *Biomed. Pharmacother.* **2023**, *162*, 114670. [[CrossRef](#)]

87. Han, B.; Dong, L.; Zhou, J.; Yang, Y.; Guo, J.; Xuan, Q.; Gao, K.; Xu, Z.; Lei, W.; Wang, J.; et al. The clinical implication of soluble PD-L1 (sPD-L1) in patients with breast cancer and its biological function in regulating the function of T lymphocyte. *Cancer Immunol. Immunother.* **2021**, *70*, 2893–2909. [[CrossRef](#)]
88. Li, Y.; Cui, X.; Yang, Y.J.; Chen, Q.Q.; Zhong, L.; Zhang, T.; Cai, R.L.; Miao, J.Y.; Yu, S.C.; Zhang, F. Serum sPD-1 and sPD-L1 as Biomarkers for Evaluating the Efficacy of Neoadjuvant Chemotherapy in Triple-Negative Breast Cancer Patients. *Clin. Breast Cancer* **2019**, *19*, 326–332.e1. [[CrossRef](#)]
89. Botticelli, A.; Pomati, G.; Cirillo, A.; Scagnoli, S.; Pisegna, S.; Chiavassa, A.; Rossi, E.; Schinzari, G.; Tortora, G.; Di Pietro, F.R.; et al. The role of immune profile in predicting outcomes in cancer patients treated with immunotherapy. *Front. Immunol.* **2022**, *13*, 974087. [[CrossRef](#)]
90. Hossen, M.J.; Yang, W.S.; Kim, D.; Aravinthan, A.; Kim, J.H.; Cho, J.Y. Thymoquinone: An IRAK1 inhibitor with in vivo and in vitro anti-inflammatory activities. *Sci. Rep.* **2017**, *7*, 42995. [[CrossRef](#)]
91. Elgohary, S.; Elkhodiry, A.A.; Amin, N.S.; Stein, U.; El Tayebi, H.M. Thymoquinone: A tie-breaker in SARS-CoV-2-infected cancer patients? *Cells* **2021**, *10*, 302. [[CrossRef](#)] [[PubMed](#)]
92. Bashmail, H.A.; Alamoudi, A.A.; Noorwali, A.; Hegazy, G.A.; Ajabnoor, G.; Choudhry, H.; Al-Abd, A.M. Thymoquinone synergizes gemcitabine anti-breast cancer activity via modulating its apoptotic and autophagic activities. *Sci. Rep.* **2018**, *8*, 11674. [[CrossRef](#)] [[PubMed](#)]
93. Rajput, S.; Kumar, B.N.P.; Dey, K.K.; Pal, I.; Parekh, A.; Mandal, M. Molecular targeting of Akt by thymoquinone promotes G1 arrest through translation inhibition of cyclin D1 and induces apoptosis in breast cancer cells. *Life Sci.* **2013**, *93*, 783–790. [[CrossRef](#)]
94. Bashmail, H.A.; Alamoudi, A.A.; Noorwali, A.; Hegazy, G.A.; Ajabnoor, G.M.; Al-Abd, A.M. Thymoquinone enhances paclitaxel anti-breast cancer activity via inhibiting tumor-associated stem cells despite apparent mathematical antagonism. *Molecules* **2020**, *25*, 426. [[CrossRef](#)] [[PubMed](#)]
95. Alobaedi, O.H.; Talib, W.H.; Basheti, I.A. Antitumor effect of thymoquinone combined with resveratrol on mice transplanted with breast cancer. *Asian Pac. J. Trop. Med.* **2017**, *10*, 400–408. [[CrossRef](#)] [[PubMed](#)]
96. Kabil, N.; Bayraktar, R.; Kahraman, N.; Mokhlis, H.A.; Calin, G.A.; Lopez-Berestein, G.; Ozpolat, B. Thymoquinone inhibits cell proliferation, migration, and invasion by regulating the elongation factor 2 kinase (eEF-2K) signaling axis in triple-negative breast cancer. *Breast Cancer Res. Treat.* **2018**, *171*, 593–605. [[CrossRef](#)]
97. Moubarak, M.M.; Chanouha, N.; Abou Ibrahim, N.; Khalife, H.; Gali-Muhtasib, H. Thymoquinone anticancer activity is enhanced when combined with royal jelly in human breast cancer. *World J. Clin. Oncol.* **2021**, *12*, 342–354. [[CrossRef](#)]
98. Parbin, S.; Shilpi, A.; Kar, S.; Pradhan, N.; Sengupta, D.; Deb, M.; Rath, S.K.; Patra, S.K. Insights into the molecular interactions of thymoquinone with histone deacetylase: Evaluation of the therapeutic intervention potential against breast cancer. *Mol. Biosyst.* **2016**, *12*, 48–58. [[CrossRef](#)]
99. Alandağ, C.; Kancağı, D.D.; Karakuş, G.S.; Çakirsoy, D.; Ovalı, E.; Karaman, E.; Yüce, E.; Özdemir, F. The effects of thymoquinone on pancreatic cancer and immune cells. *Rev. Assoc. Med. Bras.* **2022**, *68*, 1023–1026. [[CrossRef](#)]
100. Alkhattabi, N.A.; Hussein, S.A.; Tarbiah, N.I.; Alzahri, R.Y.; Khalifa, R. Thymoquinone Effect on Monocyte-Derived Macrophages, Cell-Surface Molecule Expression, and Phagocytosis. *Nutrients* **2022**, *14*, 5240. [[CrossRef](#)]
101. Ahmad, I.; Muneer, K.M.; Tamimi, I.A.; Chang, M.E.; Ata, M.O.; Yusuf, N. Thymoquinone suppresses metastasis of melanoma cells by inhibition of NLRP3 inflammasome. *Toxicol. Appl. Pharmacol.* **2013**, *270*, 70–76. [[CrossRef](#)] [[PubMed](#)]
102. Periyamayagam, S.; Arumugam, G.; Ravikumar, A.; Ganesan, V.S. Thymoquinone ameliorates NLRP3-mediated inflammation in the pancreas of albino Wistar rats fed ethanol and high-fat diet. *J. Basic Clin. Physiol. Pharmacol.* **2015**, *26*, 623–632. [[CrossRef](#)] [[PubMed](#)]
103. Guo, L.P.; Liu, S.X.; Yang, Q.; Liu, H.Y.; Xu, L.L.; Hao, Y.H.; Zhang, X.Q. Effect of Thymoquinone on Acute Kidney Injury Induced by Sepsis in BALB/c Mice. *Biomed Res. Int.* **2020**, *2020*, 1594726. [[CrossRef](#)]
104. Liu, H.; Sun, Y.; Zhang, Y.; Yang, G.; Guo, L.; Zhao, Y.; Pei, Z. Role of Thymoquinone in Cardiac Damage Caused by Sepsis from BALB/c Mice. *Inflammation* **2019**, *42*, 516–525. [[CrossRef](#)] [[PubMed](#)]
105. Pei, Z.W.; Guo, Y.; Zhu, H.L.; Dong, M.; Zhang, Q.; Wang, F. Thymoquinone Protects against Hyperlipidemia-Induced Cardiac Damage in Low-Density Lipoprotein Receptor-Deficient (LDL-R^{-/-}) Mice via Its Anti-inflammatory and Antipyroptotic Effects. *Biomed Res. Int.* **2020**, *2020*, 4878704. [[CrossRef](#)]
106. Hamdan, A.M.E.; Alharthi, F.H.J.; Alanazi, A.H.; El-Emam, S.Z.; Zaghlool, S.S.; Metwally, K.; Albalawi, S.A.; Abdu, Y.S.; Mansour, R.E.S.; Salem, H.A.; et al. Neuroprotective Effects of Phytochemicals against Aluminum Chloride-Induced Alzheimer's Disease through ApoE4/LRP1, Wnt3/ β -Catenin/GSK3 β , and TLR4/NLRP3 Pathways with Physical and Mental Activities in a Rat Model. *Pharmaceuticals* **2022**, *15*, 1008. [[CrossRef](#)]
107. Adinew, G.M.; Messeha, S.S.; Taka, E.; Badisa, R.B.; Soliman, K.F.A. Anticancer Effects of Thymoquinone through the Antioxidant Activity, Upregulation of Nrf2, and Downregulation of PD-L1 in Triple-Negative Breast Cancer Cells. *Nutrients* **2022**, *14*, 4787. [[CrossRef](#)]
108. Pelekanou, V.; Villarroel-Espindola, F.; Schalper, K.A.; Pusztai, L.; Rimm, D.L. CD68, CD163, and matrix metalloproteinase 9 (MMP-9) co-localization in breast tumor microenvironment predicts survival differently in ER-positive and -negative cancers. *Breast Cancer Res.* **2018**, *20*, 154. [[CrossRef](#)]

109. Newman, D.J.; Cragg, G.M. Natural products as sources of new drugs over the 30 years from 1981 to 2010. *J. Nat. Prod.* **2012**, *75*, 311–335. [[CrossRef](#)]
110. Cragg, G.M.; Pezzuto, J.M. Natural Products as a Vital Source for the Discovery of Cancer Chemotherapeutic and Chemopreventive Agents. *Med. Princ. Pract.* **2016**, *25*, 41–59. [[CrossRef](#)]
111. Rivera Vargas, T.; Apetoh, L. Danger signals: Chemotherapy enhancers? *Immunol. Rev.* **2017**, *280*, 175–193. [[CrossRef](#)] [[PubMed](#)]
112. Yao, M.; Fan, X.; Yuan, B.; Takagi, N.; Liu, S.; Han, X.; Ren, J.; Liu, J. Berberine inhibits NLRP3 Inflammasome pathway in human triple-negative breast cancer MDA-MB-231 cell. *BMC Complement. Altern. Med.* **2019**, *19*, 216. [[CrossRef](#)] [[PubMed](#)]
113. Faria, S.S.; Costantini, S.; de Lima, V.C.C.; de Andrade, V.P.; Rialland, M.; Cedric, R.; Budillon, A.; Magalhães, K.G. NLRP3 inflammasome-mediated cytokine production and pyroptosis cell death in breast cancer. *J. Biomed. Sci.* **2021**, *28*, 26. [[CrossRef](#)] [[PubMed](#)]
114. Nakamura, T.; Gaston, C.L.; Reddy, K.; Iwata, S.; Nishio, J. Inflammatory Biomarkers in Cancer. *Mediat. Inflamm.* **2016**, *2016*, 7282797. [[CrossRef](#)]
115. Lebreton, F.; Berishvili, E.; Parnaud, G.; Rouget, C.; Bosco, D.; Berney, T.; Lavallard, V. NLRP3 inflammasome is expressed and regulated in human islets article. *Cell Death Dis.* **2018**, *9*, 726. [[CrossRef](#)]
116. Moossavi, M.; Parsamanesh, N.; Bahrami, A.; Atkin, S.L.; Sahebkar, A. Role of the NLRP3 inflammasome in cancer. *Mol. Cancer* **2018**, *17*, 158. [[CrossRef](#)]
117. Hamarshah, S.; Zeiser, R. NLRP3 Inflammasome Activation in Cancer: A Double-Edged Sword. *Front. Immunol.* **2020**, *11*, 1444. [[CrossRef](#)]
118. Shanmugam, M.K.; Ahn, K.S.; Hsu, A.; Woo, C.C.; Yuan, Y.; Tan, K.H.B.; Chinnathambi, A.; Alahmadi, T.A.; Alharbi, S.A.; Koh, A.P.F.; et al. Thymoquinone Inhibits Bone Metastasis of Breast Cancer Cells Through Abrogation of the CXCR4 Signaling Axis. *Front. Pharmacol.* **2018**, *9*, 1294. [[CrossRef](#)]
119. Obeid, M.; Tesniere, A.; Ghiringhelli, F.; Fimia, G.M.; Apetoh, L.; Perfettini, J.L.; Castedo, M.; Mignot, G.; Panaretakis, T.; Casares, N.; et al. Calreticulin exposure dictates the immunogenicity of cancer cell death. *Nat. Med.* **2007**, *13*, 54–61. [[CrossRef](#)]
120. Elangovan, M.; Chong, H.K.; Park, J.H.; Yeo, E.J.; Yoo, Y.J. The role of ubiquitin-conjugating enzyme Ube2j1 phosphorylation and its degradation by proteasome during endoplasmic stress recovery. *J. Cell Commun. Signal.* **2017**, *11*, 265–273. [[CrossRef](#)]
121. Lenin, R.; Nagy, P.G.; Jha, K.A.; Gangaraju, R. GRP78 translocation to the cell surface and O-GlcNAcylation of VE-Cadherin contribute to ER stress-mediated endothelial permeability. *Sci. Rep.* **2019**, *9*, 10783. [[CrossRef](#)]
122. Cook, K.L.; Clarke, P.A.G.; Clarke, R. Targeting GRP78 and antiestrogen resistance in breast cancer. *Future Med. Chem.* **2013**, *5*, 1047–1057. [[CrossRef](#)] [[PubMed](#)]
123. Chou, C.-W.; Yang, R.-Y.; Chan, L.-C.; Li, C.-F.; Sun, L.; Lee, H.-H.; Lee, P.-C.; Sher, Y.-P.; Ying, H.; Hung, M.-C. The stabilization of PD-L1 by the endoplasmic reticulum stress protein GRP78 in triple-negative breast cancer. *Am. J. Cancer Res.* **2020**, *10*, 2621–2634. [[PubMed](#)]
124. Bouhleb, A.; Mosbah, B.; Abdallah, H.; Ribault, C.; Viel, R.; Mannai, S.; Corlu, A.; Abdennebi, B. Thymoquinone prevents endoplasmic reticulum stress and mitochondria-induced apoptosis in a rat model of partial hepatic warm ischemia reperfusion. *Biomed. Pharmacother.* **2017**, *94*, 964–973. [[CrossRef](#)] [[PubMed](#)]
125. Serrano Del Valle, A.; Beltrán-Visiedo, M.; de Poo-Rodríguez, V.; Jiménez-Alduán, N.; Azaceta, G.; Díez, R.; Martínez-Lázaro, B.; Izquierdo, I.; Palomera, L.; Naval, J.; et al. Ecto-calreticulin expression in multiple myeloma correlates with a failed anti-tumoral immune response and bad prognosis. *Oncoimmunology* **2022**, *11*, 2141973. [[CrossRef](#)]
126. Najibi, A.J.; Larkin, K.; Feng, Z.; Jeffreys, N.; Dacus, M.T.; Rustagi, Y.; Hodi, F.S.; Mooney, D.J. Chemotherapy Dose Shapes the Expression of Immune-Interacting Markers on Cancer Cells. *Cell. Mol. Bioeng.* **2022**, *15*, 535–551. [[CrossRef](#)]
127. Kepp, O.; Liu, P.; Zhao, L.; Plo, I.; Kroemer, G. Surface-exposed and soluble calreticulin: Conflicting biomarkers for cancer prognosis. *Oncoimmunology* **2020**, *9*, 1792037. [[CrossRef](#)] [[PubMed](#)]
128. Liu, P.; Zhao, L.; Loos, F.; Marty, C.; Xie, W.; Martins, I.; Lachkar, S.; Qu, B.; Waeckel-Énée, E.; Plo, I.; et al. Immunosuppression by Mutated Calreticulin Released from Malignant Cells. *Mol. Cell* **2020**, *77*, 748–760.e9. [[CrossRef](#)]
129. Kroemer, G.; Zitvogel, L. Subversion of calreticulin exposure as a strategy of immune escape. *Cancer Cell* **2021**, *39*, 449–451. [[CrossRef](#)]
130. Dastjerdi, M.N.; Mehdiabady, E.M.; Iranpour, F.G.; Bahramian, H. Effect of thymoquinone on P53 gene expression and consequence apoptosis in breast cancer cell line. *Int. J. Prev. Med.* **2016**, *7*, 66. [[CrossRef](#)]
131. Aslan, M.; Afşar, E.; Kırımlıoğlu, E.; Çeker, T.; Yılmaz, Ç. Antiproliferative Effects of Thymoquinone in MCF-7 Breast and HepG2 Liver Cancer Cells: Possible Role of Ceramide and ER Stress. *Nutr. Cancer* **2021**, *73*, 460–472. [[CrossRef](#)]
132. Arafa, E.S.A.; Zhu, Q.; Shah, Z.I.; Wani, G.; Barakat, B.M.; Racoma, I.; El-Mahdy, M.A.; Wani, A.A. Thymoquinone up-regulates PTEN expression and induces apoptosis in doxorubicin-resistant human breast cancer cells. *Mutat. Res. Fundam. Mol. Mech. Mutagen.* **2011**, *706*, 28–35. [[CrossRef](#)]
133. Al-Mutairi, A.; Rahman, A.; Rao, M.S. Low Doses of Thymoquinone and Ferulic Acid in Combination Effectively Inhibit Proliferation of Cultured MDA-MB 231 Breast Adenocarcinoma Cells. *Nutr. Cancer* **2021**, *73*, 282–289. [[CrossRef](#)] [[PubMed](#)]
134. Khan, A.; Aldebasi, Y.H.; Alsuhailani, S.A.; Khan, M.A. Thymoquinone augments cyclophosphamide-mediated inhibition of cell proliferation in breast cancer cells. *Asian Pacific J. Cancer Prev.* **2019**, *20*, 1153–1160. [[CrossRef](#)] [[PubMed](#)]
135. Dehghani, H.; Hashemi, M.; Entezari, M.; Mohsenifar, A. The comparison of anticancer activity of thymoquinone and nanothymoquinone on human breast adenocarcinoma. *Iran. J. Pharm. Res.* **2015**, *14*, 539–546. [[CrossRef](#)]

136. Sutton, K.M.; Greenshields, A.L.; Hoskin, D.W. Thymoquinone, a bioactive component of black caraway seeds, causes G1 phase cell cycle arrest and apoptosis in triple-negative breast cancer cells with mutant p53. *Nutr. Cancer* **2014**, *66*, 408–418. [[CrossRef](#)]
137. Sutton, K.M.; Doucette, C.D.; Hoskin, D.W. NADPH quinone oxidoreductase 1 mediates breast cancer cell resistance to thymoquinone-induced apoptosis. *Biochem. Biophys. Res. Commun.* **2012**, *426*, 421–426. [[CrossRef](#)] [[PubMed](#)]
138. Perou, C.M.; Sørlie, T.; Eisen, M.B.; Van De Rijn, M.; Jeffrey, S.S.; Ress, C.A.; Pollack, J.R.; Ross, D.T.; Johnsen, H.; Akslen, L.A.; et al. Molecular portraits of human breast tumours. *Nature* **2000**, *406*, 747–752. [[CrossRef](#)] [[PubMed](#)]
139. Prat, A.; Perou, C.M. Deconstructing the molecular portraits of breast cancer. *Mol. Oncol.* **2011**, *5*, 5–23. [[CrossRef](#)]
140. Prat, A.; Parker, J.S.; Fan, C.; Perou, C.M. PAM50 assay and the three-gene model for identifying the major and clinically relevant molecular subtypes of breast cancer. *Breast Cancer Res. Treat.* **2012**, *135*, 301–306. [[CrossRef](#)]
141. Prat, A.; Parker, J.S.; Karginova, O.; Fan, C.; Livasy, C.; Herschkowitz, J.I.; He, X.; Perou, C.M. Phenotypic and molecular characterization of the claudin-low intrinsic subtype of breast cancer. *Breast Cancer Res.* **2010**, *12*, R68. [[CrossRef](#)] [[PubMed](#)]
142. Koboldt, D.C.; Fulton, R.S.; McLellan, M.D.; Schmidt, H.; Kalicki-Veizer, J.; McMichael, J.F.; Fulton, L.L.; Dooling, D.J.; Ding, L.; Mardis, E.R.; et al. Comprehensive molecular portraits of human breast tumours. *Nature* **2012**, *490*, 61–70. [[CrossRef](#)]
143. Sun, Q.; Scott, M.J. Caspase-1 as a multifunctional inflammatory mediator: Noncytokine maturation roles. *J. Leukoc. Biol.* **2016**, *100*, 961–967. [[CrossRef](#)] [[PubMed](#)]
144. Honma, S.; Shimodaira, K.; Shimizu, Y.; Tsuchiya, N.; Saito, H.; Yanaiharu, T.; Okai, T. The influence of inflammatory cytokines on estrogen production and cell proliferation in human breast cancer cells. *Endocr. J.* **2002**, *49*, 371–377. [[CrossRef](#)] [[PubMed](#)]
145. Todorović-Raković, N.; Radulovic, M.; Vujasinović, T.; Milovanović, J.; Nikolić-Vukosavljević, D. The time-dependent prognostic value of intratumoral cytokine expression profiles in a natural course of primary breast cancer with a long-term follow-up. *Cytokine* **2018**, *102*, 12–17. [[CrossRef](#)] [[PubMed](#)]
146. Paquette, B.; Therriault, H.; Wagner, J.R. Role of interleukin-1 β in radiation-enhancement of MDA-MB-231 breast cancer cell invasion. *Radiat. Res.* **2013**, *180*, 292–298. [[CrossRef](#)]
147. Ferrari, D.; Wesselborg, S.; Bauer, M.K.A.; Schulze-Osthoff, K. Extracellular ATP activates transcription factor NF- κ B through the P2Z purinoreceptor by selectively targeting NF- κ B p65 (RelA). *J. Cell Biol.* **1997**, *139*, 1635–1643. [[CrossRef](#)]
148. Korcok, J.; Raimundo, L.N.; Ke, H.Z.; Sims, S.M.; Dixon, S.J. Extracellular nucleotides act through P2X7 receptors to activate NF- κ B in osteoclasts. *J. Bone Miner. Res.* **2004**, *19*, 642–651. [[CrossRef](#)]
149. Pantschenko, A.G.; Pushkar, I.; Anderson, K.H.; Wang, Y.; Miller, L.J.; Kurtzman, S.H.; Barrows, G.; Kreutzer, D.L. The interleukin-1 family of cytokines and receptors in human breast cancer: Implications for tumor progression. *Int. J. Oncol.* **2003**, *23*, 269–284. [[CrossRef](#)]
150. Qiu, S.Q.; Waaijer, S.J.H.; Zwager, M.C.; de Vries, E.G.E.; van der Vegt, B.; Schröder, C.P. Tumor-associated macrophages in breast cancer: Innocent bystander or important player? *Cancer Treat. Rev.* **2018**, *70*, 178–189. [[CrossRef](#)]
151. Szostakowska, M.; Trębińska-Stryjewska, A.; Grzybowska, E.A.; Fabisiwicz, A. Resistance to endocrine therapy in breast cancer: Molecular mechanisms and future goals. *Breast Cancer Res. Treat.* **2019**, *173*, 489–497. [[CrossRef](#)] [[PubMed](#)]
152. Wilson, B.E.; Shen, Q.; Cescon, D.W.; Reedijk, M. Exploring immune interactions in triple negative breast cancer: IL-1 β inhibition and its therapeutic potential. *Front. Genet.* **2023**, *14*, 1086163. [[CrossRef](#)] [[PubMed](#)]
153. De La Cruz, L.M.; Harhay, M.O.; Zhang, P.; Ugras, S. Impact of Neoadjuvant Chemotherapy on Breast Cancer Subtype: Does Subtype Change and, if so, How?: IHC Profile and Neoadjuvant Chemotherapy. *Ann. Surg. Oncol.* **2018**, *25*, 3535–3540. [[CrossRef](#)]
154. Wang, D.; Qiao, J.; Zhao, X.; Chen, T.; Guan, D. Thymoquinone Inhibits IL-1 β -Induced Inflammation in Human Osteoarthritis Chondrocytes by Suppressing NF- κ B and MAPKs Signaling Pathway. *Inflammation* **2015**, *38*, 2235–2241. [[CrossRef](#)]
155. Cui, B.W.; Bai, T.; Yang, Y.; Zhang, Y.; Jiang, M.; Yang, H.X.; Wu, M.; Liu, J.; Qiao, C.Y.; Zhan, Z.Y.; et al. Thymoquinone attenuates acetaminophen overdose-induced acute liver injury and inflammation via regulation of JNK and AMPK signaling pathway. *Am. J. Chin. Med.* **2019**, *47*, 577–594. [[CrossRef](#)]
156. Adinolfi, E.; Giuliani, A.L.; De Marchi, E.; Pegoraro, A.; Orioli, E.; Di Virgilio, F. The P2X7 receptor: A main player in inflammation. *Biochem. Pharmacol.* **2018**, *151*, 234–244. [[CrossRef](#)]
157. Lamkanfi, M.; Mueller, J.L.; Vitari, A.C.; Misaghi, S.; Fedorova, A.; Deshayes, K.; Lee, W.P.; Hoffman, H.M.; Dixit, V.M. Glyburide inhibits the Cryopyrin/Nalp3 inflammasome. *J. Cell Biol.* **2009**, *187*, 61–70. [[CrossRef](#)] [[PubMed](#)]
158. Ashcroft, F.M. ATP-sensitive potassium channelopathies: Focus on insulin secretion. *J. Clin. Investig.* **2005**, *115*, 2047–2058. [[CrossRef](#)]
159. Suddek, G.M. Thymoquinone-induced relaxation of isolated rat pulmonary artery. *J. Ethnopharmacol.* **2010**, *127*, 210–214. [[CrossRef](#)]
160. Parvardeh, S.; Sabetkasaei, M.; Moghimi, M.; Masoudi, A.; Ghafghazi, S.; Mahboobifard, F. Role of L-Arginine/NO/cGMP/KATP channel signaling pathway in the central and peripheral antinociceptive effect of Thymoquinone in rats. *Iran. J. Basic Med. Sci.* **2018**, *21*, 625–633. [[CrossRef](#)]
161. Shigaeva, M.I.; Talanov, E.Y.; Venediktova, N.I.; Murzaeva, S.V.; Mironova, G.D. A role for calreticulin in functioning of mitochondrial ATP-dependent potassium channel. *Biophysics* **2014**, *59*, 721–726. [[CrossRef](#)]
162. Adinew, G.; Messeha, S.S.; Badisa, R.; Taka, E.; Soliman, K.F.A. Thymoquinone Anticancer Effects Through the Upregulation of NRF2 and the Downregulation of PD-L1 in MDA-MB-231 Triple-Negative Breast Cancer Cells. *FASEB J.* **2022**, *36*, 4787. [[CrossRef](#)] [[PubMed](#)]

163. Heeke, A.L.; Tan, A.R. Checkpoint inhibitor therapy for metastatic triple-negative breast cancer. *Cancer Metastasis Rev.* **2021**, *40*, 537–547. [[CrossRef](#)]
164. Slater, H. FDA Approves Pembrolizumab + Chemotherapy Combination for Locally Recurrent Unresectable or Metastatic TNBC. *Oncology* **2020**, *34*, 547. [[CrossRef](#)] [[PubMed](#)]
165. Gupta, G.K.; Collier, A.L.; Lee, D.; Hofer, R.A.; Zheleva, V.; van Reesema, L.L.S.; Tang-Tan, A.M.; Guye, M.L.; Chang, D.Z.; Winston, J.S.; et al. Perspectives on triple-negative breast cancer: Current treatment strategies, unmet needs, and potential targets for future therapies. *Cancers* **2020**, *12*, 2392. [[CrossRef](#)]
166. Li, C.; Zhang, Y.; Cheng, X.; Yuan, H.; Zhu, S.; Liu, J.; Wen, Q.; Xie, Y.; Liu, J.; Kroemer, G.; et al. PINK1 and PARK2 Suppress Pancreatic Tumorigenesis through Control of Mitochondrial Iron-Mediated Immunometabolism. *Dev. Cell* **2018**, *46*, 441–455.e8. [[CrossRef](#)] [[PubMed](#)]
167. Elgohary, S.; El Tayebi, H.M. Inflammasomes in breast cancer: The ignition spark of progression and resistance? *Expert Rev. Mol. Med.* **2023**, *25*, e22. [[CrossRef](#)]
168. Cantley, L.C. The phosphoinositide 3-kinase pathway. *Science* **2002**, *296*, 1655–1657. [[CrossRef](#)]
169. Guerrero-Zotano, A.; Mayer, I.A.; Arteaga, C.L. PI3K/AKT/mTOR: Role in breast cancer progression, drug resistance, and treatment. *Cancer Metastasis Rev.* **2016**, *35*, 515–524. [[CrossRef](#)]
170. Papa, A.; Pandolfi, P.P. The pten–pi3k axis in cancer. *Biomolecules* **2019**, *9*, 153. [[CrossRef](#)]
171. Chen, J.; Jiang, C.C.; Jin, L.; Zhang, X.D. Regulation of PD-L1: A novel role of pro-survival signalling in cancer. *Ann. Oncol.* **2016**, *27*, 409–416. [[CrossRef](#)] [[PubMed](#)]
172. Wei, F.; Zhang, T.; Deng, S.C.; Wei, J.C.; Yang, P.; Wang, Q.; Chen, Z.P.; Li, W.L.; Chen, H.C.; Hu, H.; et al. PD-L1 promotes colorectal cancer stem cell expansion by activating HMGA1-dependent signaling pathways. *Cancer Lett.* **2019**, *450*, 1–13. [[CrossRef](#)] [[PubMed](#)]
173. Park, J.H.; Shin, J.M.; Yang, H.W.; Kim, T.H.; Lee, S.H.; Lee, H.M.; Cho, J.G.; Park, I.H. Cigarette smoke extract stimulates mmp-2 production in nasal fibroblasts via ros/pi3k, akt, and nf- κ b signaling pathways. *Antioxidants* **2020**, *9*, 739. [[CrossRef](#)] [[PubMed](#)]
174. Chen, J.S.; Wang, Q.; Fu, X.H.; Huang, X.H.; Chen, X.L.; Cao, L.Q.; Chen, L.Z.; Tan, H.X.; Li, W.; Bi, J.; et al. Involvement of PI3K/PTEN/AKT/mTOR pathway in invasion and metastasis in hepatocellular carcinoma: Association with MMP-9. *Hepatol. Res.* **2009**, *39*, 177–186. [[CrossRef](#)]
175. Yokoo, T.; Kitamura, M. Dual regulation of IL-1 β -mediated matrix metalloproteinase-9 expression in mesangial cells by NF-KB and AP-1. *Am. J. Physiol.* **1996**, *270*, F123–F130. [[CrossRef](#)]
176. Ruhul Amin, A.R.M.; Senga, T.; Oo, M.L.; Thant, A.A.; Hamaguchi, M. Secretion of matrix metalloproteinase-9 by the proinflammatory cytokine, IL-1 β : A role for the dual signalling pathways, Akt and Erk. *Genes Cells* **2003**, *8*, 515–523. [[CrossRef](#)]
177. Ren, P.; Wu, D.; Appel, R.; Zhang, L.; Zhang, C.; Luo, W.; Robertson, A.A.B.; Cooper, M.A.; Coselli, J.S.; Milewicz, D.M.; et al. Targeting the nlrp3 inflammasome with inhibitor mcc950 prevents aortic aneurysms and dissections in mice. *J. Am. Heart Assoc.* **2020**, *9*, e014044. [[CrossRef](#)]
178. Liu, Z.; Li, J.; Lin, S.; Wu, Y.; He, D.; Qu, P. PI3K regulates the activation of NLRP3 inflammasome in atherosclerosis through part-dependent AKT signaling pathway. *Exp. Anim.* **2021**, *70*, 488–497. [[CrossRef](#)]
179. Xu, D.; Ma, Y.; Zhao, B.; Li, S.; Zhang, Y.; Pan, S.; Wu, Y.; Wang, J.; Wang, D.; Pan, H.; et al. Thymoquinone induces G2/M arrest, inactivates PI3K/Akt and nuclear factor- κ B pathways in human cholangiocarcinomas both in vitro and in vivo. *Oncol. Rep.* **2014**, *31*, 2063–2070. [[CrossRef](#)]
180. Ma, J.; Zhang, Y.; Deng, H.; Liu, Y.; Lei, X.; He, P.; Dong, W. Thymoquinone inhibits the proliferation and invasion of esophageal cancer cells by disrupting the AKT/GSK-3 β /Wnt signaling pathway via PTEN upregulation. *Phyther. Res.* **2020**, *34*, 3388–3399. [[CrossRef](#)]
181. Hsu, H.H.; Chen, M.C.; Day, C.H.; Lin, Y.M.; Li, S.Y.; Tu, C.C.; Padma, V.V.; Shih, H.N.; Kuo, W.W.; Huang, C.Y. Thymoquinone suppresses migration of LoVo human colon cancer cells by reducing prostaglandin E2 induced COX-2 activation. *World J. Gastroenterol.* **2017**, *23*, 1171–1179. [[CrossRef](#)]
182. Haiaty, S.; Rashidi, M.R.; Akbarzadeh, M.; Bazmani, A.; Mostafazadeh, M.; Nikanfar, S.; Zibaei, Z.; Rahbarghazi, R.; Nouri, M. Correction to: Thymoquinone inhibited vasculogenic capacity and promoted mesenchymal-epithelial transition of human breast cancer stem cells. *BMC Complement. Med. Ther.* **2021**, *21*, 266. [[CrossRef](#)]
183. Tadros, S.A.; Attia, Y.M.; Maurice, N.W.; Fahim, S.A.; Abdelwahed, F.M.; Ibrahim, S.; Badary, O.A. Thymoquinone Suppresses Angiogenesis in DEN-Induced Hepatocellular Carcinoma by Targeting miR-1-3p. *Int. J. Mol. Sci.* **2022**, *23*, 15904. [[CrossRef](#)]
184. Alshyarba, M.; Otfi, H.; Al Fayi, M.; A Dera, A.; Rajagopalan, P. Thymoquinone inhibits IL-7-induced tumor progression and metastatic invasion in prostate cancer cells by attenuating matrix metalloproteinase activity and Akt/NF- κ B signaling. *Biotechnol. Appl. Biochem.* **2021**, *68*, 1403–1411. [[CrossRef](#)]
185. Liou, Y.F.; Hsieh, Y.S.; Hung, T.W.; Chen, P.N.; Chang, Y.Z.; Kao, S.H.; Lin, S.W.; Chang, H.R. Thymoquinone inhibits metastasis of renal cell carcinoma cell 786-o-si3 associating with downregulation of MMP-2 and u-pa and suppression of PI3K/src signaling. *Int. J. Med. Sci.* **2019**, *16*, 686–695. [[CrossRef](#)] [[PubMed](#)]
186. Arumugam, P.; Subramanian, R.; Priyadharsini, J.V.; Gopalswamy, J. Thymoquinone inhibits the migration of mouse neuroblastoma (Neuro-2a) cells by down-regulating MMP-2 and MMP-9. *Chin. J. Nat. Med.* **2016**, *14*, 904–912. [[CrossRef](#)] [[PubMed](#)]
187. Yang, J.; Kuang, X.R.; Lv, P.T.; Yan, X.X. Thymoquinone inhibits proliferation and invasion of human nonsmall-cell lung cancer cells via ERK pathway. *Tumor Biol.* **2015**, *36*, 259–269. [[CrossRef](#)] [[PubMed](#)]

188. Kolli-Bouhafs, K.; Boukhari, A.; Abusnina, A.; Velot, E.; Gies, J.P.; Lugnier, C.; Rondé, P. Thymoquinone reduces migration and invasion of human glioblastoma cells associated with FAK, MMP-2 and MMP-9 down-regulation. *Investig. New Drugs* **2012**, *30*, 2121–2131. [[CrossRef](#)]
189. Markham, A. Alpelisib: First Global Approval. *Drugs* **2019**, *79*, 1249–1253. [[CrossRef](#)]
190. Ghallab, A.M.; Eissa, R.A.; El Tayebi, H.M. CXCR2 Small-Molecule Antagonist Combats Chemoresistance and Enhances Immunotherapy in Triple-Negative Breast Cancer. *Front. Pharmacol.* **2022**, *13*, 862125. [[CrossRef](#)]
191. Boro, M.; Balaji, K.N. CXCL1 and CXCL2 Regulate NLRP3 Inflammasome Activation via G-Protein–Coupled Receptor CXCR2. *J. Immunol.* **2017**, *199*, 1660–1671. [[CrossRef](#)] [[PubMed](#)]
192. Wan, Y.; Ge, K.; Zhou, W.; Lu, J.; Jia, C.; Zhu, H. C-X-C chemokine receptor 2 (Cxcr2) promotes hepatocellular carcinoma immune evasion via regulating programmed death-ligand 1 (PD-L1). *Biol. Chem.* **2021**, *402*, 729–737. [[CrossRef](#)] [[PubMed](#)]
193. Ashour, A.E.; Abd-Allah, A.R.; Korashy, H.M.; Attia, S.M.; Alzahrani, A.Z.; Saquib, Q.; Bakheet, S.A.; Abdel-Hamied, H.E.; Jamal, S.; Rishi, A.K. Thymoquinone suppression of the human hepatocellular carcinoma cell growth involves inhibition of IL-8 expression, elevated levels of TRAIL receptors, oxidative stress and apoptosis. *Mol. Cell. Biochem.* **2014**, *389*, 85–98. [[CrossRef](#)] [[PubMed](#)]
194. Gupta, A.; Dagar, G.; Chauhan, R.; Sadida, H.Q.; Almarzooqi, S.K.; Hashem, S.; Uddin, S.; Macha, M.A.; Akil, A.S.A.-S.; Pandita, T.K.; et al. Cyclin-dependent kinases in cancer: Role, regulation, and therapeutic targeting. In *Control of Cell Cycle & Cell Proliferation*; Donev, R., Ed.; Advances in Protein Chemistry and Structural Biology; Elsevier: Amsterdam, The Netherlands, 2023; Volume 135, pp. 21–55. Available online: <https://www.sciencedirect.com/science/article/pii/S1876162323000135> (accessed on 16 March 2023).
195. Rezaeian, A.H.; Inuzuka, H.; Wei, W. Insights into the aberrant CDK4/6 signaling pathway as a therapeutic target in tumorigenesis. *Adv. Protein Chem. Struct. Biol.* **2023**, *135*, 179–201.
196. Pham, D.V.; Raut, P.K.; Pandit, M.; Chang, J.H.; Katila, N.; Choi, D.Y.; Jeong, J.H.; Park, P.H. Globular adiponectin inhibits breast cancer cell growth through modulation of inflammasome activation: Critical role of sestrin2 and AMPK signaling. *Cancers* **2020**, *12*, 613. [[CrossRef](#)] [[PubMed](#)]

Disclaimer/Publisher’s Note: The statements, opinions and data contained in all publications are solely those of the individual author(s) and contributor(s) and not of MDPI and/or the editor(s). MDPI and/or the editor(s) disclaim responsibility for any injury to people or property resulting from any ideas, methods, instructions or products referred to in the content.